Virulence strategies of an insect herbivore and oomycete plant pathogen converge on host E3 SUMO ligase SIZ1 to suppress plant immunity

Liu, S[1]., Lenoir, C.J.G.[1,2]*, Amaro, T.M.M.M.[2]*§, Rodriguez, P.A[2¶]. Huitema, E. [1]**, Bos, J.I.B. [1,2]**

*these authors contributed equally
**Co-corresponding author

[1] Division of Plant Sciences, School of Life Sciences, University of Dundee, Dundee, DD2 5DA
[2]Cell and Molecular Sciences, The James Hutton Institute, Invergowrie, Dundee, DD2 5DA

§ current address: Tecnológico de Antioquia – Institución Universitaria Calle 78B No. 72A - 220, Medellín, Colombia
¶ current address: Helmholtz Zentrum München, Deutsches Forschungszentrum für Gesundheit und Umwelt (GmbH), Ingolstädter Landstr. 1, 85764 Neuherberg

**Corresponding Authors:

Jorunn I.B. Bos, PhD
Division of Plant Sciences, School of Life Sciences, University of Dundee
Cell and Molecular Sciences, James Hutton Institute
Invergowrie, Dundee
DD2 5DA
United Kingdom

j.bos@dundee.ac.uk

E. Huitema
Division of Plant Sciences, School of Life Sciences, University of Dundee
Invergowrie, Dundee
DD2 5DA
United Kingdom

e.huitema@dundee.ac.uk

Abstract

Plant parasites must colonise and reproduce on plants to survive. In most cases, active immune responses, triggered by (conserved) microbe-encoded molecules keep invaders at bay. Post-translational modifications (PTMs) of proteins are vital for contextual regulation and integration of plant immune responses. Pathogens and pests secrete proteins (effectors) to interfere with plant immunity through modification of host target functions and disruption of immune signalling networks. Importantly, molecular virulence strategies of distinct pathogens converge on a small set of regulators with central roles in plant immunity. The extent of convergence between pathogen and herbivorous insect virulence strategies is largely unexplored. Here we report that effectors from the oomycete pathogen, *Phytophthora capsici*, and the major aphid pest, *Myzus persicae* target the host immune regulator SIZ1, an E3 SUMO ligase. SIZ1-regulated immunity in Arabidopsis against bacterial pathogens is known to require the resistance protein SNC1, and signalling components PAD4 and EDS1. We show that SIZ1 functions as a negative regulator of plant immunity to aphids and an oomycete pathogen. However, this immune regulation is independent of SNC1, PAD4 and EDS1-signalling pointing to the presence of a novel SIZ1-mediated immune signalling route. Our results suggest convergence of distinct pathogen and pest virulence strategies on an E3 SUMO ligase that negatively regulates plant immunity.

Introduction

The plant immune system is complex, featuring different classes of receptors to detect pathogens and pests and initiate a multi-layered defence responses. Pattern recognition receptors (PRRs) recognize conserved pest and pathogen molecules, called pathogen associated molecular patterns (PAMPs), to activate immune responses and fight off the intruder (Jones and Dangl, 2006; Monaghan and Zipfel, 2012). Pathogens and pests deliver an arsenal of effector proteins inside their host to counter these and other plant defence pathways to promote effector-triggered susceptibility (ETS) through modulation of host protein activities. In addition, these effectors likely contribute to effective infection or infestation strategies by promoting the release of nutrients to support pathogen or pest growth. Another layer of plant immunity may be activated upon recognition of these effectors, or their activities, by nucleotide-binding leucine-rich repeat proteins (NLRs), which usually is associated with the activation of a Hypersensitive Response (HR). Given that plants carefully balance energy allocation between growth, development and reproduction, any effective immune responses need to be appropriate and controlled (Huot et al., 2014).

The identification of effector host targets and their effector-induced modification(s) can reveal the mechanistic basis of virulence and the biological processes that lead to susceptibility. Moreover, the identification of effector host targets for a range of pathogens pointed to convergence on key

host proteins. For example, Avr2 from the fungal pathogen *Cladosporium fulvum*, EPIC1 and EPIC2B from the oomycete *Phytophthora infestans*, and Gr-VAP1 from the plant-parasitic nematode *Globodera rostochiensis* target the same defense protease Rcr3^{pim} in tomato (Song et al., 2009; Lozano-Torres et al., 2012). In addition, the effector repertoires of distinct plant pathogens, such as the bacterium *Pseudomonas syringae*, oomycete *Hyaloperonospora arabidopsidis*, and the ascomycete *Golovinomyces orontii* disrupt key components of immune signalling networks (Mukhtar et al., 2011; Weßling et al., 2014). Specifically, transcription factor TCP14 is targeted by effectors from *P. syringae*, *H. arabidopsidis* and *Phytophthora capsici*, and contributes to plant immunity (Stam et al., 2013; Weßling et al., 2014). These findings suggest that molecular virulence strategies have evolved independently in distinct pathogens and converged on a small set of regulators with central roles in immunity.

While over the past decades our understanding of pathogen virulence strategies and susceptibility has increased dramatically, the extent with which host targets of plant-herbivorous insects overlap with other pathogens remains to be investigated. Effector biology has recently emerged as a new area in plant-herbivorous insect interactions research, leading to the identification of effector repertoires in several species (Carolan et al., 2009; Bos et al., 2010; Kaloshian and Walling, 2016; Thorpe et al., 2018; Rao et al., 2019), several host targets, and insights into their contribution to the infestation process (Rodriguez et al., 2017; Chaudhary et al., 2019; Wang et al., 2019; Xu et al., 2019). These studies support an extension of the effector paradigm in plant-microbe interactions to plant-herbivorous insect interactions. Whether plant pathogenic microbes and insects adopt similar strategies to attack and reprogram their host to redirect immune responses is yet to be determined.

Here, we show that *Myzus persicae* (aphid) effector, Mp64, and *P. capsici* (oomycete) effector CRN83_152 (also called PcCRN4) (Stam et al., 2013; Mafurah et al., 2015), associate with the immune regulator SIZ1 in the plant nucleus. SIZ1 stability and cell death activation in *N. benthamiana* are differentially affected by these effectors, suggesting these proteins feature distinct activities via this immune regulator. SIZ1 is an E3 SUMO ligase involved in abiotic and biotic stress responses, including Salicylic Acid (SA)-mediated innate immunity and EDS1/PAD4-mediated Resistance gene signalling (Miura et al., 2005; Catala et al., 2007; Lee et al., 2007; Miura et al., 2007; Jin et al., 2008; Miura et al., 2009; Ishida et al., 2012; Lin et al., 2016). Additionally, SIZ1 regulates plant immunity partially through the immune receptor SNC1 (Gou et al., 2017) and controls the trade-off between SNC1-dependent immunity and growth in Arabidopsis at elevated temperature (Hammoudi et al., 2018). By using Arabidopsis knock-out lines and gene silencing in *N. benthamiana* we show that SIZ1 functions as a negative regulator of plant immunity to aphids and an oomycete pathogen. However, this immune regulation is independent of SNC1-signalling pointing to the presence of a novel SIZ1-mediated immune signalling route. Our results

suggest that the effector target convergence principle can be extended to herbivorous insects and raise important questions about mechanisms of action.

Results

Aphid effector Mp64 and oomycete effector CRN83_152 interact with AtSIZ1 and NbSIZ1, and Mp64 stabilizes SIZ1 *in planta*.

To gain novel insight into pathogen and pest effectors, we successfully applied yeast-two-hybrid screens to identify candidate host targets (Rodriguez et al., 2017). We identified the E3 SUMO ligase SIZ1 in screens against a *N. benthamiana* library (generated from aphid infested and *P. capsici* infected leaves) with *M. persicae* (aphid) effector Mp64 and *P. capsici* (oomycete) effector CRN83_152 as baits. Mp64 was screened against an estimated $5x10^6$ cDNAs and revealed 2 independent prey clones with an insert showing similarity to SIZ1, whilst the effector CRN83_152 screen of $4x10^6$ yeast transformants, identified 3 independent prey clones with an insert similar to SIZ1. All putative interactors identified in the two effector screens are summarized in Table S1. Since all NbSIZ1 (*N. benthamiana* SIZ1) prey clones from the Mp64 and CRN83_152 screens were partial-length, we designed primers to amplify and clone the full-length NbSIZ1. Although we were unable to amplify NbSIZ1 based on the two best BLAST hits against the *N. benthamiana* genome database due to poor primer annealing at the 3' end, we successfully amplified NbSIZ1 sequences based on the 3' end of SIZ1 sequences from *N. attenuata* (XP_019237903) and *N. tomentosiformis* (XP_018631066). The full-length NbSIZ1 sequence we cloned was identical to our partial yeast prey clones and NbSIZ1 database sequences, except for a 27 amino acid insertion at position 225-252. A direct comparison between NbSIZ1 and the well characterised AtSIZ1 showed 60% identity between proteins (Supplementary

Fig.S1). Given that AtSIZ1 is well characterised and helps regulate plant immunity (Miura et al., 2005; Catala et al., 2007; Lee et al., 2007; Hammoudi et al., 2018), we included AtSIZ1 in our efforts to further validate effector-SIZ1 interactions and characterise the role of SIZ1 in immunity to aphids and oomycetes. It should be noted that whilst Arabidopsis is a host for *M. persicae*, this plant species is not a natural host for *P. capsici*. We first tested whether Mp64 and CRN83_152 interact with full-length NbSIZ1 and AtSIZ1 in yeast. Whilst yeast reporter assays showed interaction of Mp64 with both full-length SIZ1 versions (Supplementary Fig. S2), we were unable to obtain yeast co-transformants expressing both CRN83_152 and full-length SIZ1 in repeated transformation experiments that included transformation controls. We also included a mutant of CRN83_152, called CRN83_152_6D10 (Amaro et al., 2018), which does not trigger CRN-cell death activation but retains virulence activity, in co-transformation experiments with similar results.

To test for *in planta* effector-SIZ1 interactions, we co-expresssed GFP-Mp64 and GFP-CRN83_152_6D10 with either AtSIZ1-myc or NbSIZ1-myc in *N. benthamiana* (Fig. 1A and B). Immunoprecipitation of both effectors resulted in the co-purification of NbSIZ1, suggestive of an association *in planta* (Fig. 1B). Co-immunoprecipitation of the effectors with AtSIZ1 gave similar results with the exception of CRN83_152, where no AtSIZ1 was detected (Fig. 1A). It should be noted that CRN83_152 activates cell death in these assays, leading to protein degradation as reflected by a weaker Ponceau staining of Rubisco (Fig. 1A). We found that input samples consistently showed an increased intensity of the band corresponding to the AtSIZ1 and NbSIZ1 proteins upon co-expression with Mp64 but not CRN83-152_6D10. To test whether Mp64 indeed stabilizes SIZ1 *in planta*, we performed co-expression assays of both effectors with SIZ1 in parallel in three independent biological replicates. Western blot analyses showed that AtSIZ1 levels were higher than NbSIZ1 levels among all replicates. Also, we consistently observed an increase in SIZ1 protein levels in the presence of Mp64 compared to the GFP-GUS control (Fig. 1C, Supplementary Fig. S3), indicating that Mp64 stabilizes SIZ1 *in planta*.

CRN83_152_6D10 but not Mp64 enhances AtSIZ1 triggered cell death in *N. benthamiana*

When performing transient expression assays in *N. benthamiana* with AtSIZ1 and NbSIZ1, we observed the onset of cell death starting from 3 days after infiltration specifically upon expression of AtSIZ1. We investigated whether co-expression of the aphid and oomycete effectors with SIZ1 would either enhance or reduce this cell death activation. In the absence of any effectors, AtSIZ1 consistently activated cell death from 3-4 days after infiltration, whereas only occasional microscopic cell death was visible in infiltration sites expressing NbSIZ1. Both AtSIZ1 and NbSIZ1 fusion proteins, with a C-terminal RFP tag, were detectable in transient expression assays (Supplementary Fig. S5). While co-expression of Mp64 with SIZ1 did not affect the cell death phenotype, co-expression of CRN83_152_6D10 with AtSIZ1 led to a stronger cell death response compared to the AtSIZ1 and CRN83_152_6D10 controls (Fig. 2; Supplementary Fig. S4). These data suggest that CRN83_152_6D10 but not Mp64 enhances AtSIZ1-triggered cell death.

Nuclear aphid effector Mp64 enhances Arabidopsis susceptibility to *M. persicae*

While the nuclear PcCRN83_152 effector from *P. capsici* was previously shown to be essential for pathogen virulence and promotes plant susceptibility (Stam et al., 2013; Mafurah et al., 2015), the role of aphid effector Mp64, which was previously identified as a candidate effector in *A. pisum* and *M. persicae* through bioinformatics pipelines (Carolan et al., 2011; Thorpe et al., 2016; Boulain et al., 2018), in plant-aphid interactions is unknown. Mp64 is a protein of unknown function with a predicted nuclear localisation based on ProteinPredict (Yachdav et al., 2014) and NLStradamus (Nguyen Ba et al., 2009), and Mp64 homologs are present in other aphid species (Supplementary

Fig. S5). We investigated the subcellular localisation of Mp64 by confocal microscopy of *N. benthamiana* leaves transiently expressing GFP-Mp64 (lacking the predicted signal peptide). Imaging of epidermal cells expressing Mp64 revealed accumulation of GFP-Mp64 in the nucleus and nucleolus, with no signal detectable in the cytoplasm (Fig. 3A). In addition, we observed dots within the nucleoplasm corresponding to GFP-Mp64. Nuclear localisation of GFP-Mp64 was confirmed upon co-localisation with the nuclear marker Histone 2B (H2B) (Fig. 3B).

To confirm whether Mp64 can affect host susceptibility to aphids, we generated Arabidopsis transgenic lines expressing the mature Mp64 protein driven by the 35S promoter. Arabidopsis lines expressing Mp64 (Supplementary Fig. S6A) showed no developmental or growth phenotypes (Supplementary Fig. S6B) and were subjected to aphid fecundity assays. Two age-synchronized *M. persicae* aphids were placed on transgenic Mp64 lines and Col-0 control plants, and progeny was counted after 10 days. The average number of aphids on two independent transgenic Mp64 lines (25.6 and 29.5) was 31-34% higher than on the Col-0 control (Mann-Whitney U test, $p<0.05$; Fig. 2C), indicating that Mp64 enhances Arabidopsis host susceptibility to *M. persicae*.

To test whether Mp64 also affects *P. capsici* infection, we transiently over-expressed Mp64 and a vector control in *N. benthamiana* and challenged infiltration sites with a zoospore suspension (Supplementary Fig. S7). In contrast to the *P. capsici* effector CRN83_152, aphid effector Mp64 did not enhance host susceptibility to *P. capsici*, suggesting that these effectors have distinct virulence activities despite sharing SIZ1 as a virulence target.

Effectors Mp64 and CRN83_152 co-localise with SIZ1 in the host nucleus

Since both Mp64 and CRN83_152 are nuclear effectors, and their host interacting protein SIZ1 is reported to localise and function in the plant nucleus (Miura et al., 2005), we determined whether the effectors co-localise with SIZ1 in this subcellular compartment. We performed confocal imaging of *N. benthamiana* leaves transiently co-expressing SIZ1-mRFP and GFP-effector fusions. In line with previous reports, mRFP signal corresponding to both AtSIZ1 and NbSIZ1 was visible in the plant nucleoplasm, along with distinct speckles in the nucleolus (Fig. 4; Supplementary Fig. S8). Expression of full-length SIZ1-RFP was confirmed by western blotting (Supplementary Fig. S9). In addition, GFP signal corresponding to GFP-Mp64 and CRN83_152 was detectable in the nucleus. Mp64 or CRN83_152 did not affect the localisation of SIZ1 and similarly, SIZ1 did not affect the localisation of the effectors (Fig. 4; Supplementary Fig. S8). Our data suggests that effectors Mp64 and CRN83_152 associate with SIZ1 in the host nucleus.

Silencing of *NbSIZ1* reduces *N. benthamiana* host susceptibility to *P. capsici*

To assess the contribution of SIZ1 to immunity in a *P. capsici* host species, we made use of Virus Induced Gene Silencing (VIGS) in *N. benthamiana* (Ratcliff et al., 2001; Lu et al., 2003). Our TRV-*NbSIZ1* construct, designed to silence *NbSIZ1*, reduced transcripts levels by around 60% compared with plants expressing the TRV-GFPfrag control (a fragment of GFP). Silenced plants showed a slight reduction in growth compared with the TRV-GFPfrag control and cell death in older leaves (Supplementary Fig. S10A and C). In our hands, VIGS assays based on TRV in *N. benthamiana* are incompatible with aphid assays (TRV infection causes aphids to die), therefore, we only performed infection assays with *P. capsici* on *NbSIZ1* silenced plants. Detached leaves were used for *P. capsici* infection assays based on zoospore droplet inoculations, followed by lesion size diameter measurements. *P. capsici* lesion size on *NbSIZ1* silenced leaves was significantly reduced 2-4 days after inoculation when compared to control plants (Mann-Whitney U test, $p<0.0001$; Fig. 5; Supplementary Fig. S10B). These results indicate that NbSIZ1 contributes to host susceptibility to this oomycete plant pathogen, possibly by negatively regulating plant immunity.

Loss-of-function mutation *siz1-2* in Arabidopsis leads to enhanced resistance to *M. persicae* and *P. capsici*

Since AtSIZ1 negatively regulates plant innate immunity in Arabidopsis to the bacterial plant pathogen *Pseudomonas syringae* pv. Tomato DC3000 (Pst) (Lee et al., 2007), we tested whether this also applies to interactions with *M. persicae* and *P. capsici*. We performed aphid performance assays, based on fecundity measurements, as well as *P. capsici* infection assays on the Arabidopsis loss-of-function mutant *siz1-2*. Given that siz1-2 mutants have a dwarf phenotype, associated with SA hyper-accumulation, we included Arabidopsis line *siz1-2*/NahG, in which this phenotype is (partially) abolished (Lee et al., 2007). While Arabidopsis is a host for the aphid *M. persicae,* only few *P. capsici* isolates infect Arabidopsis under controlled environmental conditions and high levels of inoculum (Wang et al., 2013), suggesting that Arabidopsis is not a natural host. Aphid performance assays showed a significant reduction in fecundity on the *siz1-2* and *siz1-2*/*NahG* lines compared to the Col-0 (ANOVA, $p<0.0001$; Fig. 6A) and *NahG* controls (ANOVA, $p<0.01$; Fig. 6A), respectively, with only few aphids surviving on the *siz1-2* line. The *siz1-2* reduced susceptibility to aphids is largely maintained in the *NahG* background, implying that this phenotype is largely independent of SA accumulation.

For *P. capsici* infection assays, plants were spray inoculated with a zoospore solution and the percentage of symptomatic leaves was counted 10 days later. The percentage of symptomatic *siz1-2* leaves was reduced by 83% compared with the Col-0 control (ANOVA, $p<0.0001$; Fig. 5B, Supplementary Fig. S11). We did not observe a difference in *P. capsici* infection levels between

the *NahG* line and Col-0, but did note a slight increase in infection on *siz1/NahG* compared to the *NahG* background (ANOVA, p<0.01; Fig. 6B, Supplementary Fig. S11).

Arabidopsis s*iz1-2* enhanced resistance to *M. persicae* and *P. capsici* is independent of SNC1, EDS1 and PAD4

EDS1, PAD4 and SNC1 are required for *siz1-2* enhanced resistance to *P. syringae* pv tomato DC3000 (Lee et al., 2007; Gou et al., 2017; Hammoudi et al., 2018). To explore whether these signalling components also contribute to *siz1-2* enhanced resistance to aphids and *P. capsici*, we performed aphid infestation and infection assays on Arabidopsis *siz1-2/eds1-2*, *siz1-2/pad4-1* and *siz1-2/snc1-11* double mutants.

Aphid infestation on the *siz1-2/eds1-2* mutant was reduced by 75% compared with the *eds1-2* mutant (ANOVA, p<0.0001, Fig. 6C), and was comparable to *siz1-2* (Fig. 6C), suggesting that the reduced susceptibility of *siz1-2* to aphids is independent of EDS1. In addition, aphid fecundity was reduced on *siz1-2/pad4-1* by around 65% compared with the *pad4-1* mutant (ANOVA, p<0.0001, Fig. 5C), and was comparable to *siz1-2* (Fig. 6C). These data suggest that *siz1-2* reduced susceptibility to aphids is also independent of PAD4.

In line with previous reports (Wang et al., 2013) the *eds1-2* and *pad4-1* mutants were less resistant to *P. capsici* than Col-0 (ANOVA, p<0.0001, Fig. 6D, Supplementary Fig. S10), indicating EDS1 and PAD4 contribute to Arabidopsis nonhost resistance to this pathogen. The percentage of symptomatic *siz1-2/eds1-2* and *siz1-2/pad4-1* leaves was around 60% and 55% less compared to the *eds1-2* (ANOVA, p<0.0001, Fig. 6D, Supplementary Fig. S11) and *pad4-1* (ANOVA, p<0.0001, Fig. 5D, Supplementary Fig. S10) mutants, respectively. Similar to our aphid data, *siz1-2* enhanced resistance to *P. capsici* is not fully dependent on EDS1 and PAD4, with *siz1-2* showing an enhanced resistance phenotype in the *eds1-2* and *pad4-1* mutant background and when compared to the appropriate controls (*eds1-2* and *pad4-1* respectively).

Aphid fecundity on *siz1-2/snc1-11* was approximately 85% reduced compared with the *snc1-11* control (ANOVA, p<0.0001), and was comparable to *siz1-2* (Fig. 6E), suggesting that *siz1-2* reduced susceptibility to aphids is independent of SNC1. The *siz1-2/snc1-11* double mutant also showed enhanced resistance to *P. capsici*, with 55% less symptomatic leaves compared to the *snc1-11* mutant (ANOVA, p<0.0001, Fig. 5B, Supplementary Fig. S10). The percentage of symptomatic leaves on *siz1-2/snc1-11* was slightly higher compared with the *siz1-2* mutant (ANOVA, p<0.05, Fig. 6B, Supplementary Fig. S11). With the *siz1-2* enhanced resistance to *P. capsici* largely maintained in the *snc1-11* background, this phenotype is likely independent of the immune receptor SNC1. Overall, *siz1-2* enhanced resistance to both *M. persicae* and *P. capsici* is independent of signalling components previously implicated in SIZ1 immune functions.

Arabidopsis *siz1-2* reduced susceptibility to aphids involves phloem resistance factors

To shed light on the potential mechanism underlying reduced susceptibility to *M. persicae* in the Arabidopsis *siz1-2* mutant, we monitored aphid probing and feeding behaviour using the Electrical penetration graph (EPG) technique. Global analysis of all 80 recorded EPG parameters showed that the feeding activities of *M. persicae* on *siz1-2* are not significantly different compared with those on Col-0 control plants (MANOVA, p=0.054, Table 1.). However, feeding patterns within the vascular tissue differed significantly as indicated by 17 relevant parameters (Table 1). The average duration aphids spent on a single phloem salivation event (E1) on the *siz1-2* mutant was two times longer, and the length of time aphids spent on phloem salivation and then phloem ingestion (E12) was 3 times shorter than on the Col-0 control. Furthermore, aphids spent less time ingesting phloem sap (E2) on the *siz1-2* mutant than on the Col-0 control, and the ratio of time aphids spent ingesting phloem sap relative to the length of time probing plant tissue (E2/C) was significantly lower (Mann-Whitney U test, $p<0.05$; Fig. 7). Additional aphid feeding parameters, which underline vascular-related resistance against aphids are displayed in Table 1. Overall, aphids have more difficulties feeding on phloem sap of the *siz1-2* mutant than that of Col-0 plants, suggesting that the reduced susceptibility phenotype is at least partly associated with plant phloem factors.

Discussion

Pathogen infection strategies involve extensive modification of host cell biology, which rely on the modulation of hubs that control plant immunity. In this study, we show that effectors from an herbivorous insect and oomycete plant pathogen target the host E3 SUMO ligase SIZ1. Our findings suggest that the virulence strategies of two plant parasites with distinct evolutionary histories and lifestyles, convergence on an important host immune component.

Our finding that SIZ1 is a key target of distinct plant parasites is in line with a recent study on the cyst nematode *Globodera pallida,* which shows that effector GpRbp1 associates with potato SIZ1 *in planta* (Diaz-Granados et al., 2019). Importantly StSIZ1 emerged as a negative regulator of immunity in plant-nematode interactions (Diaz-Granados et al., 2019), but the signalling requirements for this immunity have not yet been reported. We propose that SIZ1 is a hub that regulates immunity to a broad range of plant parasites, including herbivorous insects. Indeed, Arabidopsis *siz1-2* plants show enhanced immunity not only upon pathogen infection as reported here (Fig. 5) and previously (Lee et al., 2007) but also upon aphid infestation. In contrast to *siz1-2* enhanced resistance to *P. syringae pv. tomato* DC3000, which is dependent on SA, EDS1, PAD4 and SNC1, we find that resistance to the aphid *M. persicae* and the oomycete *P. capsici* is largely independent from these signalling components. These results point to an as yet unknown SIZ1-dependent signalling pathway that regulates plant immunity. Although PAD4 has been reported to play an important role in plant defence against *M. persicae* (Pegadaraju et al., 2007), in line with

Lei et al. (Lei et al., 2014), we did not observe an enhanced susceptibility phenotype of Arabidopsis *pad4-1* in our aphid performance assays.

A reduction of SA levels in the *NahG* line did not enhance defence against the aphid *M. persicae* (this study and previous reports (Pegadaraju et al., 2007; Lei et al., 2014)), nor did this reduce nonhost resistance to the oomycete *P. capsici,* in contrast to an earlier report by Wang et al. (Wang et al., 2013). However, we did observe a trend towards reduced resistance of the transgenic NahG line to *P. capsici*, but this reduction was not statistically significant and may be less pronounced due to differences in experimental set-up and infection conditions compared to Wang et al (Wang et al., 2013). Arabidopsis defence to insect herbivores is mediated predominantly through JA-signalling, whereas defence against (hemi-)biotrophic pathogens tend to rely on SA-signalling (Howe and Jander, 2008; Pieterse et al., 2012). In the Arabidopsis-*M. persicae* interaction, *siz1-2* reduced susceptibility is largely independent of SA accumulation, with the *siz1-2/NahG* line being more resistant to aphids than the *NahG* control and Col-0 (Fig. 5). Therefore, and in contrast to Lee et al.(Lee et al., 2007), SIZ1-regulated immunity to aphids is independent of SA-signalling. Our EPG analyses of aphid probing and feeding behaviour on Arabidopsis *siz1-2* suggest the presence of resistance factors that act against aphids in the phloem. Phloem-mediated defences against aphids include the occlusion of sieve elements, which prevents aphids from ingesting phloem sap, as well as deterrents in the phloem sap (Mayoral et al., 1996; Will and van Bel, 2006; Medina-Ortega and Walker, 2015). Interestingly, the Arabidopsis *siz1-2* mutant features changes in cell division, cell expansion and secondary cell wall formation, including reduced secondary cell wall thickening (Miura et al., 2010; Liu et al., 2019). Aphid feeding can trigger changes in cell wall composition that are associated with defences (Rasool et al., 2017), and therefore changes in cell wall formation can be responsible for altered susceptibility. However, reduced cell wall thickening most likely would lead to a reduction in defence against aphids rather than an increase as observed in the *siz1-2* mutant, and we found no evidence of altered stylet pathways or probing indicative of cell wall-associated defences.

With SIZ1 comprised of several conserved domain involved in different stress responses (Cheong et al., 2009) it is possible that Mp64 and CRN83-152 target different protein regions and functions. Arabidopsis and *N. benthamiana* SIZ1 domains include the SAP (scaffold attachment factor A/B/acinus/PIAS) domain, PINIT (proline-isoleucine-asparagine-isoleucine-threonine) domain, an SP-RING (SIZ/PIAS-RING) domain, SXS motif (serine-X-serine), and a PHD (plant homeodomain). Functional analyses, using a set of (deletion) mutants revealed that these domains contribute differently to the wide range of SIZ1 functions in both abiotic and biotic stress (Cheong et al., 2009). The SP-RING domain of AtSIZ1 contributes to the nuclear localisation, SUMOylation activity, as well as the regulation of SA levels and associated plant defence responses. This domain is the suggested SIZ1 target site of the nematode effector GpRbp1 to interfere with SA-mediated defences (Diaz-Granados et al., 2019). Our Arabidopsis-*M. persicae* interaction assays

though suggest that SIZ1 may also contribute to immunity in a SA-independent manner where other domains may play an important role. Interestingly, SIZ1-mediated SUMOylation is involved in regulating sugar signalling independent of SA (Castro et al., 2015; Castro et al., 2018), with the *siz1-2* mutant showing reduced starch levels and increased expression of starch and sucrose catabolic genes. Aphid infestation affects sugar metabolism as reflected for example by an increase in sucrose and starch in infested Arabidopsis plants (Singh et al., 2011). With sugars in phloem sap also being the main aphid food source, it will be interesting to further explore a possible link between the role of SIZ1 in regulating sugar signaling and host susceptibility.

Although our data support a key role for SIZ1 in plant immunity to *P. capsici* and *M. persicae* that is targeted during infection and infestation, the mechanism by which Mp64 and CRN83-152 affect SIZ1 is to be elucidated. The presence of host SIZ1 is required for infestation/infection as knock-out of *AtSIZ1* and knock-down of *NbSIZ1* result in reduced host susceptibility phenotypes. Therefore, we propose that Mp64 and CRN83-152 redirect and perhaps enhance SIZ1 function rather than inhibit it. In line with this, our Arabidopsis transgenic lines expressing Mp64 do not show a reduced growth phenotype similar to the *siz1-2* mutant (Supplementary Fig S4). Moreover, expression of CRN83-152 but not Mp64 in *N. benthamiana* led to an increase in *P. capsici* infection. Moreover, Mp64 but not CRN83-152_6D10 enhanced stability of AtSIZ1 protein while CRN83-152_6D10 but not Mp64 increased AtSIZ1-triggered cell death in *N. benthamiana*. Based on these observations, we propose that while both virulence strategies have converged onto SIZ1, their mechanisms of action are distinct. In this context, we cannot rule out that additional candidate targets of Mp64 and CRN83-152 identified in our Y2H screens (Supplementary Table S1) explain our observed differences in effector virulence activities.

As an E3 SUMO ligase, SIZ1 is required for SUMOylation of a range of substrates including chromatin modifiers, coactivators, repressors, and transcription factors that are associated with biotic and abiotic stress responses (Rytz et al., 2018). Similar to ubiquitination, SUMOylation involves three key steps (Verma et al., 2018). First, the SUMO precursor is cleaved and the SUMO moiety is linked to an SUMO-activating enzyme (E1). Activated SUMO is then transferred to the SUMO-conjugating enzyme (E2), after which it is linked to target substrates with the help of SUMO-ligases (E3). In the SUMO cycle, SUMO proteases are responsible for processing of the SUMO precursor and release of SUMO from target substrates. Whether the cell death triggered by AtSIZ1 upon transient expression in *N. benthamiana* is linked to E3 SUMO ligase activity remains to be investigated. It is possible that AtSIZ1 expression in a different plant species than Arabidopsis leads to mis-targeting of substrates, and subsequently activation of cell death. Although Mp64 did not enhance the cell death triggered by AtSIZ1, this effector did increase SIZ1 protein stability. Similarly, the effector AVR3a from *P. infestans* interacts with and stabilizes the E3 ubiquitin ligase CMPG1, likely by modifying its activity, to suppress plant immunity (Bos et al., 2010). The mechanism underlying the stabilization of SIZ1 by Mp64 is yet unclear. However, we

hypothesize that increased stability of SIZ1, which functions as an E3 SUMO ligase, likely leads to increased SUMOylation activity towards its substrates and will likely affect SIZ1 complex formation with other key regulators of plant immunity.

SUMOylation of target proteins plays an important role in plant immunity and is known to be targeted as part of bacterial plant pathogen infection strategies (Verma et al., 2018)). For example, effector XopD from *Xanthomonas campestris pv. vesicatoria* (*Xcv*) functions as a SUMO protease inside host cells to modulate host defence signalling (Hotson et al., 2003; Kim et al., 2008). SUMOylation sites are predicted in Mp64 (Supplementary Fig. S3) and CRN83-152 (1 SUMO interaction motif: SVEKGANILSVEVPGCDVD; 2 SUMOylation sites: VKMLIEVKREVKSAS and WSHPQFEK*******) using prediction software GPS-SUMO (Zhao et al., 2014). Possibly, these effectors are themselves SIZ1 substrates, and their SUMOylation may be required for virulence activity. Our data suggest that modification of host SUMOylation is a common strategy of plant parasites to enable host colonization, and that the targeting strategies have evolved independently in distinct plant-feeding organisms including herbivorous insects. In future work, a detailed analyses of changes in the SIZ1-dependent host plant SUMOylome will be needed to understand how distinct plant parasites promote virulence through SIZ1 targeting.

Materials and Methods

Plants and growth conditions

Nicotiana benthamiana plants were grown in a greenhouse with 16h of light and temperature of 25° during the daytime.

Transgenic Arabidopsis lines *siz1-2*, *eds1-2*, *pad4-1*, *NahG*, *siz1-2*/*NahG*, *siz1-2/eds1-2*, *siz1-2/pad4-1* were kindly provided by Dr H.A. van den Burg, The University of Amsterdam. *Arabidopsis thaliana* plants were grown in growth chambers with an 8h light/16h dark cycle at 22°/20° (day/night), with a light intensity of 100-200 µmol/m^{-2} s^{-1} and relative humidity of 60%.

Aphid rearing and *P. capsici* growth conditions

M. persicae (JHI_genotype O (Thorpe et al., 2018)) was maintained on oil seed rape (*Brassica napus*) plants in a Perspex growth chamber, with 12h light, and a temperature of 17°C and 50% relative humidity.

P. capsici isolate LT1534 was maintained on V8 agar cubes at room temperature. For zoospore collection, P. capsici LT1534 was grown on V8 agar plates at 25°.

Plasmid construction

The coding sequence of Mp64, lacking the region encoding the N-terminal signal peptide, was amplified from *M. persicae* (JHI_genotype O) cDNA by PCR with gene-specific primers DONR-Mp64_F and DONR-Mp64_Rev (Supplementary Table S2.) The amplicon was cloned into entry vector pDONR207 (Invitrogen) using Gateway cloning technology. Cloning of the *Phythophthora capsici* effector CRN83_152 and the CRN83_152_6D10 mutant was previously described (Stam et al., 2013; Amaro et al., 2018). For *in planta* expression, both effectors were cloned into destination vector pB7WGF2 (N-terminal GFP tag) (Karimi et al., 2002).

An entry clone carrying *AtSIZ1* was kindly provided by Dr H.A. van den Burg, The University of Amsterdam. *NbSIZ1* was amplified from *N. benthamiana* cDNA with gene-specific primers NbSIZ1-attB1 and NbSIZ1-attB2 or NbSIZ1-attB2-nostop (Supplementary Table S2). Amplicons were cloned into entry vector pDONR207 (Invitrogen) using Gateway technology. For *in planta* expression, *AtSIZ1* and *NbSIZ1* were cloned into destination vectors pB7FWG2 (C-terminal GFP tag)(Karimi et al., 2002), pK7RWG2 (C-terminal mRFP tag, Karimi et al., 2005), and pGWB20 (C-terminal 10xMyc tag) (Nakagawa et al., 2007).

Yeast-two-hybrid assays

Yeast two hybrid screening of effectors against a *N. benthamiana* library was based on the Dualsystems Y2H system (Dual Systems Biotech) and performed following the manufacturer's instructions. Bait vectors (pLex-N) carrying effector sequences (lacking the signal peptide encoding sequence) were transformed into yeast strain NMY51. Yeast cells expressing effectors were transformed with a *N. benthamiana* prey library. This prey library was generated in pGAD-HA from cDNA obtained from a combination of healthy leaves, leaves infected with *P. capsici*, and leaves infested with aphids. Transformants were selected on synthetic dropout media plates lacking leucine, histidine and tryptophan (-LTH) with addition of 2.5mM 3-amino-1,2,4-triazole (3-AT). Yeast colonies selected on –LTH media were subjected to the β-galactosidase reporter assays according to manufacturer's instructions (Dual Systems Biotech). The inserts of selected yeast colonies were sequenced and analysed. The Mp64/CRN83_152-NbSIZ1 interaction was validated in yeast by independent co-transformation experiments and reporter assays.

Generation of Arabidopsis transgenic lines by floral dipping

Arabidopsis thaliana wild type (Col-0) were grown in the greenhouse under long-day conditions (16h of light) until flowering. The flowers of plant were dipped 3 times (one-week interval) in the agrobacterium strain GV3101 suspension of OD_{600} =0.8-2 carrying binary plasmid pB7WG2-Mp64 or empty vector pB7WG2. T1 transformants were selected using 100µg/ml BASTA (Glufosinate-

ammonium) spray, and T2 seed were selected Murashige Skoog media containing 10μg/mL BASTA. Homozygous T3 plants (predicted single insertion based on 3:1 segregation in T2) were used for aphid performance experiments. Internal primers Mp64 (Mp64-int-F and Mp64-int-Rev) were designed to confirm the presence of Mp64 in transgenic Arabidopsis by RT-PCR.

SIZ1 cell death assays

For SIZ1 cell death assay, agrobacterium GV3101 cultures carrying C-terminal RFP tagged AtSIZ1, NbSIZ1 or GUS were infiltrated into *N. benthamiana* leaves with an OD600 of 0.3, together with culture containing silencing suppressor p19 (OD600=0.1).

For co-expression assays, mixtures of agrobacterium cultures carrying N-terminal GFP tagged Mp64, CRN83_152_6D10 or GUS with cultures carrying C-terminal RFP tagged AtSIZ1, NbSIZ1 or GUS respectively were injected into *N. benthamiana* leaves with an OD600 of 0.3 for each construct (p19 was added with OD600=0.1). The cell death level was scored at 4-7 days post inoculation using a scale of 0-3 based on the severity of the phenotype. Infiltration site were scored for no symptoms (score 0), chlorosis with localized cell death (score 1), less than 50% of the site showing visible cell death (score 2), over 50% of the infiltration site showing cell death (score 3).

Infection assays on *N. benthamiana* leaves transiently expressing effectors

Phytophthora capsici growth assays were performed on *N. benthamiana* leaves expressing CRN83-152_6D10, Mp64 or the vector control upon agroinfiltration (OD600=0.3 each). Two days after infiltration, leaves were drop inoculated with 5 μL of zoospore solution (50,000 spores/mL) from *P. capsici* strain LT1534. Lesion diameters were measured at 2 days post-inoculation.

Pathogen and pest infection/infestation assays on Arabidopsis

Two 2-day old *M. persicae* nymphs (age-synchronized) were placed on 4-6-week old Arabidopsis plants. The plants were placed in a large plastic tube sealed with a mesh lid and placed in a growth cabinet (8h of light, 22/20° for day/night, 60% humidity). The numbers of aphids per plant were counted 10 days post infestation.

P. capsici isolate LT1534 was grown in V8 agar plate for 3 days in the dark at 25° and exposed to continuous light for 2 days to stimulate sporulation. Sporangia was dislodged and collected with ice-cold water. The sporangia suspension was incubated under light for 30-45min to promote zoospore release. For Arabidopsis infection, 4-6 weeks old plants were spray-inoculated with a spore suspension of 100,000 spores/ml. The percentage of infected leaves was scored 8 days after spray inoculation.

Statistical analyses were carried out by using R studio Version 1.2.5001 running R-3.6.1. A linear mixed effects model, with experimental block and biological replicate incorporated as random factors, was used for aphid fecundity assays. A linear mixed effects model, with biological replicates as a random factor, was used for *P. capsici* infection assays. ANOVA was used to analyse the final models, by using emmeans package calculating the Least Squares Means as a post hoc test.

Virus-induced gene silencing assays

Tobacco rattle virus (TRV)-based virus-induced gene silencing (VIGS) was used to silence *NbSIZ1* in *N. benthamiana*. The VIGS construct was generated by cloning a 249-bp fragment of *NbSIZ1*, amplified with primers Sumo_Vigs_Phusion_Frag3_F and Sumo_Vigs_Phusion_Frag3_R (Supplementary Table S2). To generate a TRV-only control, a GFP fragment was amplified using the primers eGFP_Fw and eGFP_Rv. Amplified fragments were cloned into the Tobacco Rattle Virus vector (pTRV2) (Lu et al., 2003) using the In-Fusion HD cloning kit (Clontech). Agrobacterium strains containing desired pTRV2 constructs were co-infiltrated with strains carrying pTRV1 at OD_{600}=0.5 into 4-leaf-stage *N. benthamiana* plants. Three weeks post infiltration, leaves at the same position of different plants were detached for quantification of *NbSIZ1* transcripts by qRT-PCR and *P.capsici* infection assays. Six independent plants were used for each VIGS construct in each replicated experiment, with a total of three replicated experiments. For infection assays on silenced plants, leaves were drop-inoculated with 5µL of zoospore suspension (50,000 spores per mL) of *P. capsici* strain LT1534, or for data corresponding to Supplementary Fig S7 with 10ul of zoospore suspension (100,000). Lesion diameter was recorded 2-3 days post inoculation. Data analyses was carried out by using R studio Version 1.2.5001 running R-3.6.1. Group comparison was conducted by Mann-Whitney U test for non-normally distributed data.

Confocal microscopy

Agrobacterium strain carrying desired constructs were infiltrated individually or in combination in *N. benthamiana* plants with an OD_{600} of 0.1. *N. benthamiana* cells were imaged at 1-2 days post infiltration using a Leica TCS SP2 AOBS, Zeiss 710 confocal microscopes with HC PL FLUOTAR 63X0.9 and HCX APO L U-V 40X0.8 water-dipping lenses. GFP was excited with 488 nm from an argon laser, and emissions were detected between 500 and 530 nm. The excitation wavelength for mRFP was 561 nm and emissions were collected from 600 to 630 nm. *N. benthamiana* Histone (H2B) fused to mRFP was used as a nuclear marker (Goodin et al., 2007). Single optical section images or z-stacks images were collected from leaf cells those have relatively low expression level to minimize the potential artefacts. Images were projected and processed using the Image J 1.52p-Fiji (Wayne Rasband, National Institute of Health, USA). Further figure generation was processed with Adobe Photoshop CS5.1.

Protein Extractions, co-Immunoprecipitation and stability assays

Agrobacterium strain GV3101 expressing N-terminal GFP-tagged Mp64/CRN83_152/CRN83_152_6D10 and C-terminal 10xMyc-tagged AtSIZ1/NbSIZ1 were co-infiltrated in *N. benthamiana* leaves with an OD_{600} of 0.3 with addition of p19 (OD_{600}=0.1). Leaf samples were harvested 48 hours post infiltration. For detection of GFP and RFP fusion proteins used in localization experiments, Laemmli loading buffer (addition of 10mM DTT) was directly added ground leaf samples followed by SDS-PAGE and western blotting. For CO-IP, equal amounts of plant material were extracted in GTEN buffer (10% glycerol, 25 mM Tris-HCl PH=7.5, 150 mM NaCl, 1mM EDTA) supplemented with protease inhibitor (S8820, Sigma-Aldrich), 2% PVPP, 0.1% NP-40 detergent and fresh 10mM DTT. Samples were incubated for 10 min on ice. The lysate was centrifuged at 14460g for 3 times, 4min/each time and then the supernatants were subjected to CO-IP with GFP-Trap®-M magnetic beads (Chromotek) for affinity binding of GFP-fused proteins. Western blotting was performed with a monoclonal GFP antibody raised in mouse (Sigma-Aldrich, cat. no. G1546) and a monoclonal cMyc antibody raised in mouse (Santa Cruz, cat. no. SC-40) at 1:3000 dilution, followed by anti-mouse Ig-HRP antibody (Sigma-Aldrich, cat. no. A9044) at 1:5000 dilution to detect corresponding epitopes. To assess SIZ1 protein levels in the presence/absence of effectors, equal amount of leaf tissue was extracted in GTEN extraction buffer as described above. Prior to western blotting, total protein extracts were run on an SDS-PAGE gel followed by Coomassie staining. Equal amounts of protein extract were run on SDS-PAGE gels followed by western blotting. Upon antibody incubation, chemiluminescence was detected using a Syngene G:Box XT4 camera.

RNA extraction and Quantitative RT-PCR

Total RNA was extracted by using RNeasy Mini Kit (Qiagen) with a following DNase I treatment (Invitrogen™) from VIGS *N. benthamiana*. 1 µg RNA was reverse-transcribed using SuperScript III reverse transcriptase (Sigma-Aldrich, UK) following the manufacturer's protocol. RT-qPCR experiment was designed following the MIQE guidelines (Bustin et al., 2009) with gene specific primers (Supplementary Table S2). Herein EF1α (accession number: TC19582 (At5g60390)) and PP2A (accession number: TC21939 (At1g13320)) (Liu et al., 2012) were used as reference genes. For PCR amplification, GoTaq® RT-qPCR system (Promega, UK) was used on a StepOne™ Real-Time PCR Machine (Applied Biosystems, UK). In each reaction, 12.5 µl reactions with a final concentration of 1x GoTaq® qPCR Master Mix, 1µM of each primer, 1.4 mM MgCl2, 2.4 µM CXR reference dye and a cDNA quantity of approx. 25 ng. The PCR program was set as follows: 95° for 15 mins followed by 40 cycles of 15s at 95°, 30s at 60°, and 30s at 72°. A melting curve was generated at the end of the PCR program and $2^{-\Delta\Delta Ct}$ value (Livak and Schmittgen, 2001) was calculated to determine the relative expression of *NbSIZ1*. Three technical replicates were performed in each run and three biological replicates were carried out throughout the experiment.

538 **Electrical penetration graph (EPG) monitoring of aphid feeding**

539 We used the EPG technique (Tjallingii, 1978) (monitor the probing and feeding behaviour of *M.*
540 *persicae* on Arabidopsis Col-0 and the *siz1-2* mutant using a Giga-4 DC-EPG device with 1 Giga Ω
541 resistance (EPG systems, The Netherlands). Experimental set up was described by Leybourne et
542 al. (2019)(Leybourne et al., 2019). Software Stylet +D was used for data collection (EPG systems,
543 The Netherlands). A total of 12 and 15 successful recordings were obtained from aphids feeding
544 on Col-0 and *siz1-2* Arabidopsis plants, respectively. Different waveform patterns were observed,
545 such as np (non-probing), C (stylet penetration/pathway), pd (intercellular punctures), E1 (saliva
546 secretion into phloem), E2 (saliva secretion and passive phloem ingestion), F (mechanical
547 penetration difficulty) or G (xylem ingestion) phases (Tjallingii, 1988; Alvarez et al., 2006). R studio
548 Version 1.2.5001 running R-3.6.1 was used for statistical analyses. A permutated MANOVA was
549 fitted to the dataset for global assessing of aphid feeding behavior, and Mann-Whitney U test was
550 used to carry out pairwise comparisons.

551

552 **Acknowledgements**

553 We thank Dr. Daniel Leybourne for advice on statistical and EPG analyses, Dr. Petra Boevink for
554 advice on confocal microscopy, and Dr. Harrold van den Burg for providing the various Arabidopsis
555 *siz1-2* mutant lines. We also thank Dr. Nicholas Birch (The James Hutton Institute) for allowing us
556 to use the EPG equipment. This work was supported by the Biotechnology and Biological Sciences
557 Research Council (grant no. BB/J005258/1 to JIBB), the European Research Council (grant no.
558 APHIDHOST-310190 to JIBB and 310901_RETRaIN to EH), and funding from the China
559 Scholarship Council (CSC to SL). *Phytophthora capsici* cultures were held at The James Hutton
560 Institute under license PH\6\2015. The authors declare no conflict of interest.

Figures and Tables

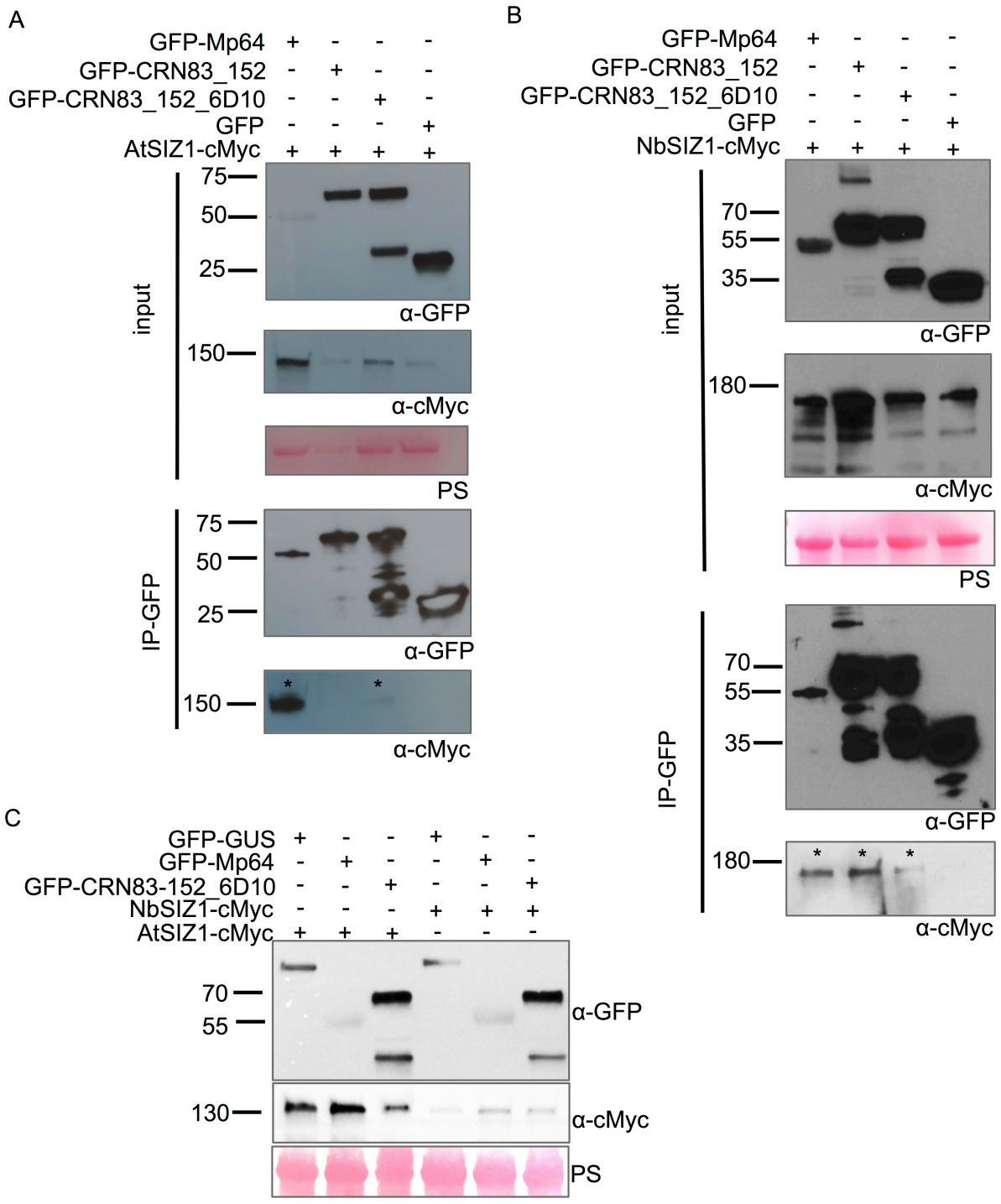

Fig. 1. *Myzus persicae* effector Mp64 and *Phytophthora capsici* effector CRN83_152 associate with SIZ1 from Arabidopsis and *Nicotiana benthamiana*.

(A) Immunoprecipitation (IP) of protein extracts from agroinfiltrated leaves using GFP-Trap confirmed that AtSIZ1-cMyc(10x) associates with GFP-Mp64 and GFP-CRN83_152_6D10, but not with the GFP control.

(B) Immunoprecipitation (IP) of protein extracts from agroinfiltrated leaves using GFP-Trap confirmed that NbSIZ1-cMyc(10x) associates with GFP-Mp64, GFP-CRN83_152 and GFP-CRN83_152_6D10, but not with the GFP control. Protein size markers are indicated in kD, and

protein loading is shown upon ponceau staining of membranes. Experiments were repeated at least three times with similar results.

(C) Stabilisation of SIZ1 by Mp64. Western blot analyses of protein extracts from agroinfiltrated leaves expressing combinations of GFP-GUS, GFP-Mp64 and GFP-CRN83_152_6D10 with AtSIZ1-myc or NbSIZ1-myc. Protein size markers are indicated in kD, and equal protein amounts upon transfer is shown upon ponceau staining (PS) of membranes. Blot is representative of three biological replicates , which are all shown in supplementary Fig. S3. The selected panels shown here are cropped from Rep 1 in supplementary Fig. S3.

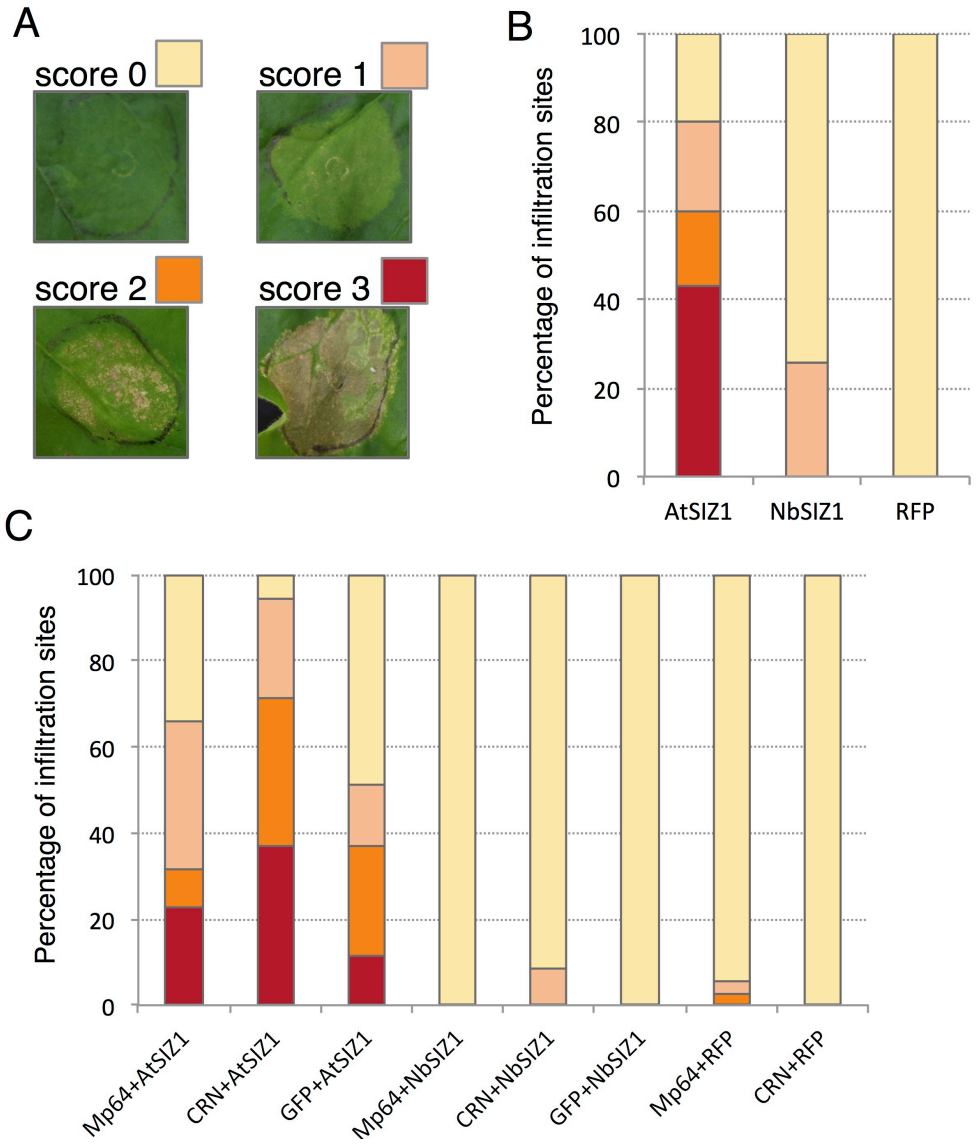

Fig. 2. SIZ1-triggered cell death in *N. benthamiana* is enhanced by CRN83_152_6D10 but not Mp64.

(A) Scoring overview of infiltration sites for SIZ1-triggered cell death. Infiltration site were scored for no symptoms (score 0), chlorosis with localized cell death (score 1), less than 50% of the site showing visible cell death (score 2), more than 50% of the infiltration site showing cell death (score 3).

(B) Bar graph showing the proportions of infiltration sites with different levels of cell death upon expression of AtSIZ1, NbSIZ1 (both with a C-terminal RFP tag) and an RFP control. Graph represents data from a combination of 3 biological replicates of 11-12 infiltration sites per experiment (n=35). Data was collected 7 days after infiltration.

(C) Bar graph showing the proportions of infiltration sites with different levels of cell death upon expression of SIZ1 (with C-terminal RFP tag) either alone or in combination with aphid effector Mp64 or Phytophthora capsica effector CRN83_152_6D10 (both effectors with GFP tag), or a GFP control. Data was collected 7 days after infiltration. Graph represent data from a combination of 3 biological replicates of 11-12 infiltration sites per experiment (n=35).

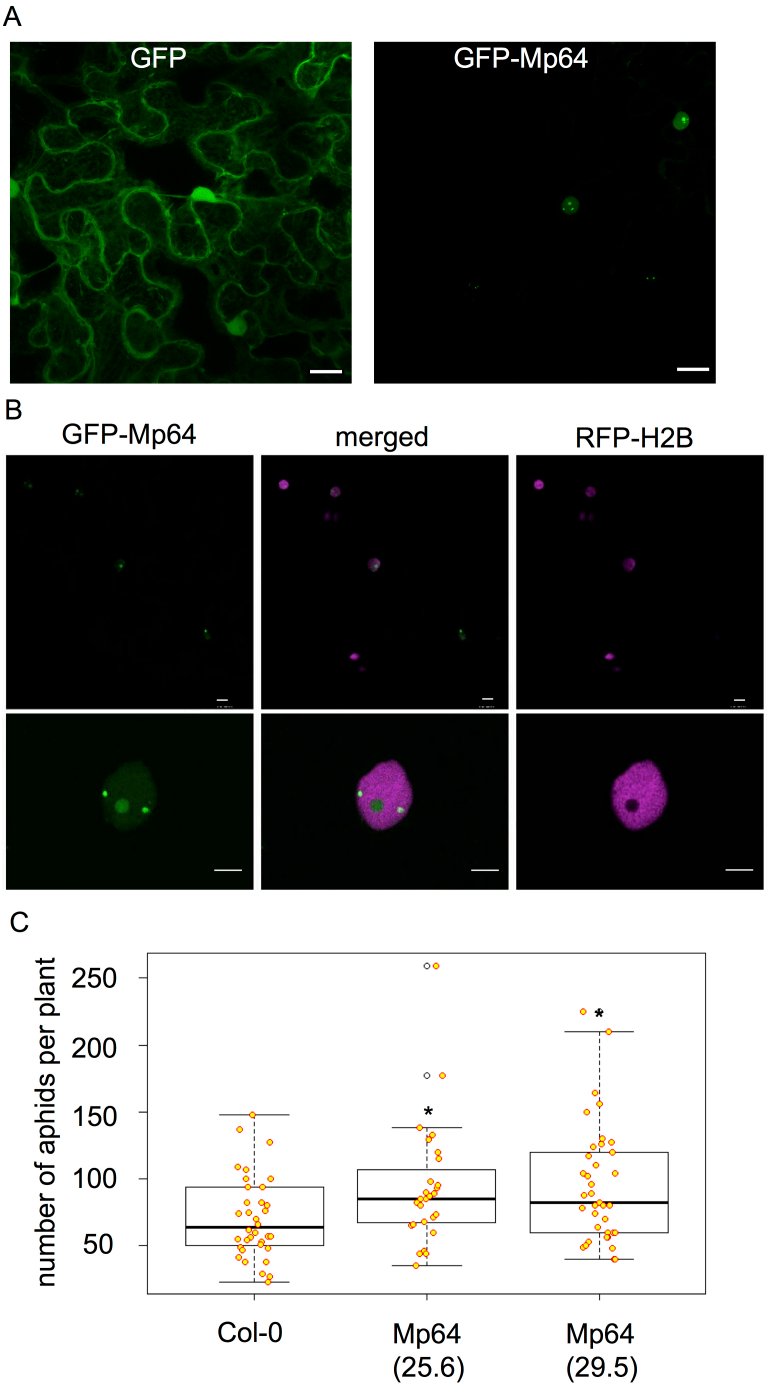

Fig. 3. Constitutive ectopic expression of nuclear aphid effector Mp64 in Arabidopsis enhances susceptibility to *Myzus persicae*.

(A) Confocal images showing nuclear localisation of aphid effector Mp64 in host *Nicotiana benthamiana*. Leaves transiently expressing GFP-Mp64 and histone marker RFP-Histone 2B (H2B), a nuclear marker, were used for confocal imaging 2 days after agroinfiltration. Images in the upper panel were collected as z-stack projection and those in the lower panel were collected as single optical sections through nuclei of cells ectopically overexpressing Mp64. Scale bar represents 10μm.

(B) Two Arabidopsis transgenic lines, 25.6 and 29.5, were challenged with two apterous adult aphids. Total numbers of aphids per plant were counted 10 days post infestation. The boxplot displays the distribution of datapoints from three independent biological replicates (n=10 per replicate). The black line within the box represents the median. The top and bottom edges of the box indicate upper quantile and lower quantile. The datapoints out of the upper and lower extreme

of the whisker are outliners. Asterisks denote significant difference between treatments and control (Mann-Whitney U test, $p<0.05$).

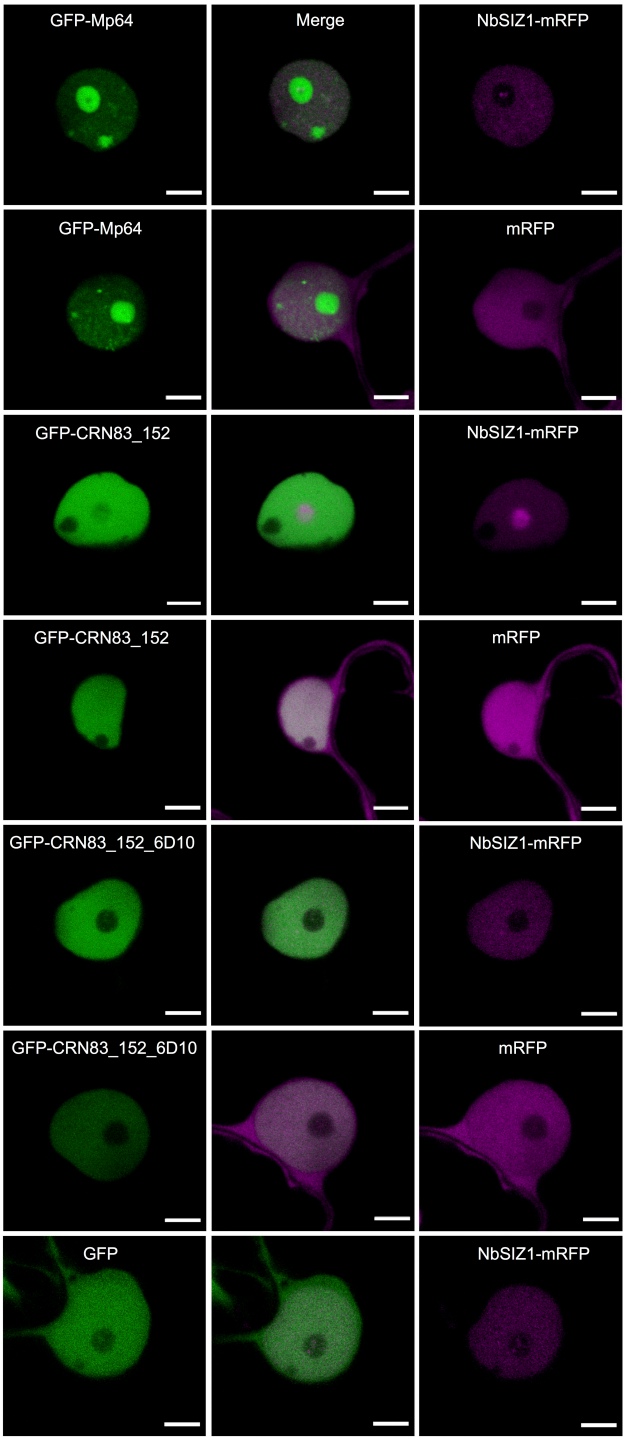

Fig. 4. Effectors Mp64 and CRN83_152 co-localize with NbSIZ1 in the host nucleus.

Leaves transiently expressing GFP-Mp64, GFP-CRN83_152 or GFP-CRN83_152_6D10 in combination with RFP or NbSIZ1-RFP were used for confocal imaging 2 days after agroinfiltration. Images show single optical sections through nuclei co-expressing the GFP-effector with NbSIZ1-RFP or RFP control. Scale bars represent 5 µm.

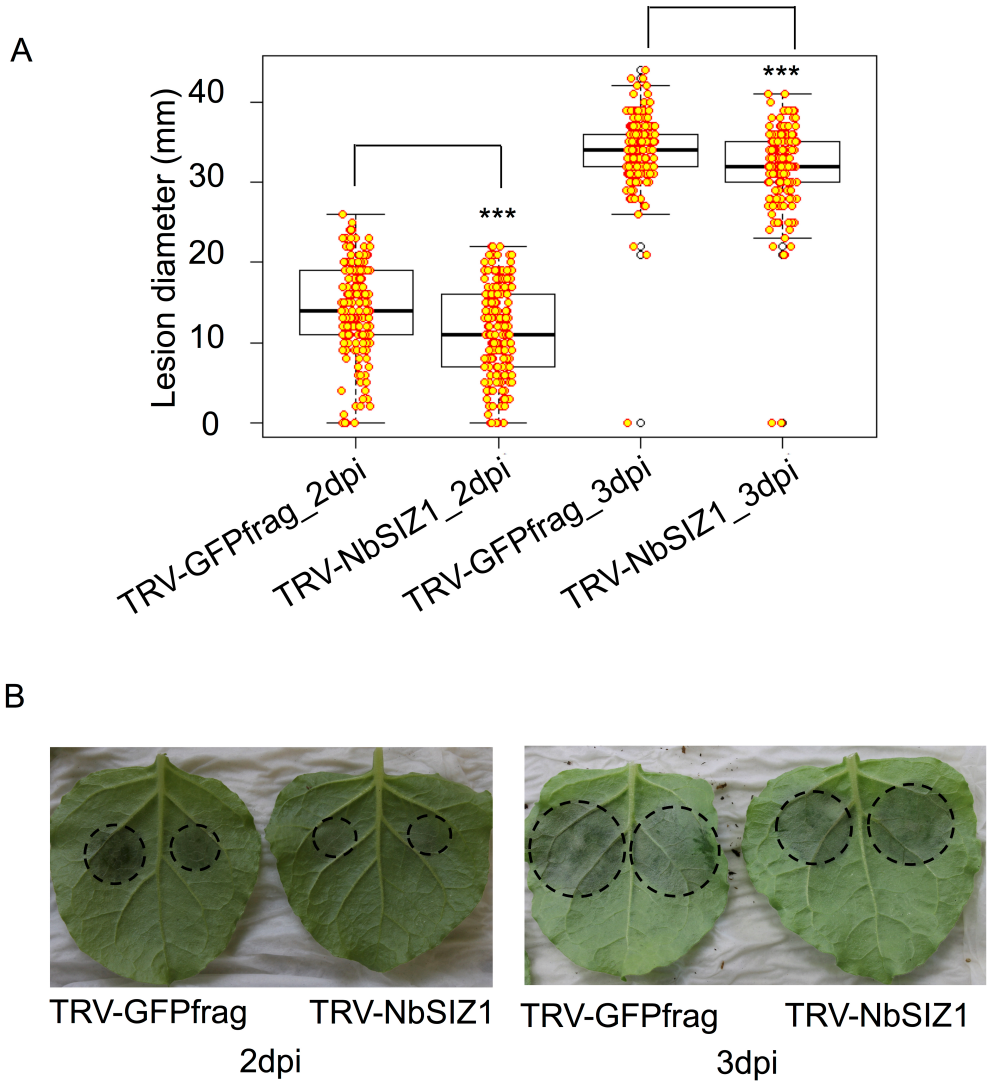

Fig. 5. Virus-induced gene silencing of *NbSIZ1* reduces host susceptibility to *Phytophthora capsici*.

(A) Boxplot showing the lesion diameter of *P. capsici* infection sites on *Nicotiana benthamiana* control (TRV-GFPfrag) or *NbSIZ1*-silenced plants (TRV-NbSIZ1). 5ul of zoospore suspension (50,000 spores/ml) was drop-inoculated on *N. benthamiana* leaves. Data was collected 2 and 3 days post inoculation (dpi) from three biological replicates (n=48 per biological replicate). Asterisks denote significant difference between the GFPfrag control and *NbSIZ1*-silenced plants (Mann-Whitney U test, $p<0.0001$).

(B) Representative images of *NbSIZ1*-silenced and GFPfrag control leaves 2 days and 3 days post inoculation (dpi) with *P. capsici* zoospores.

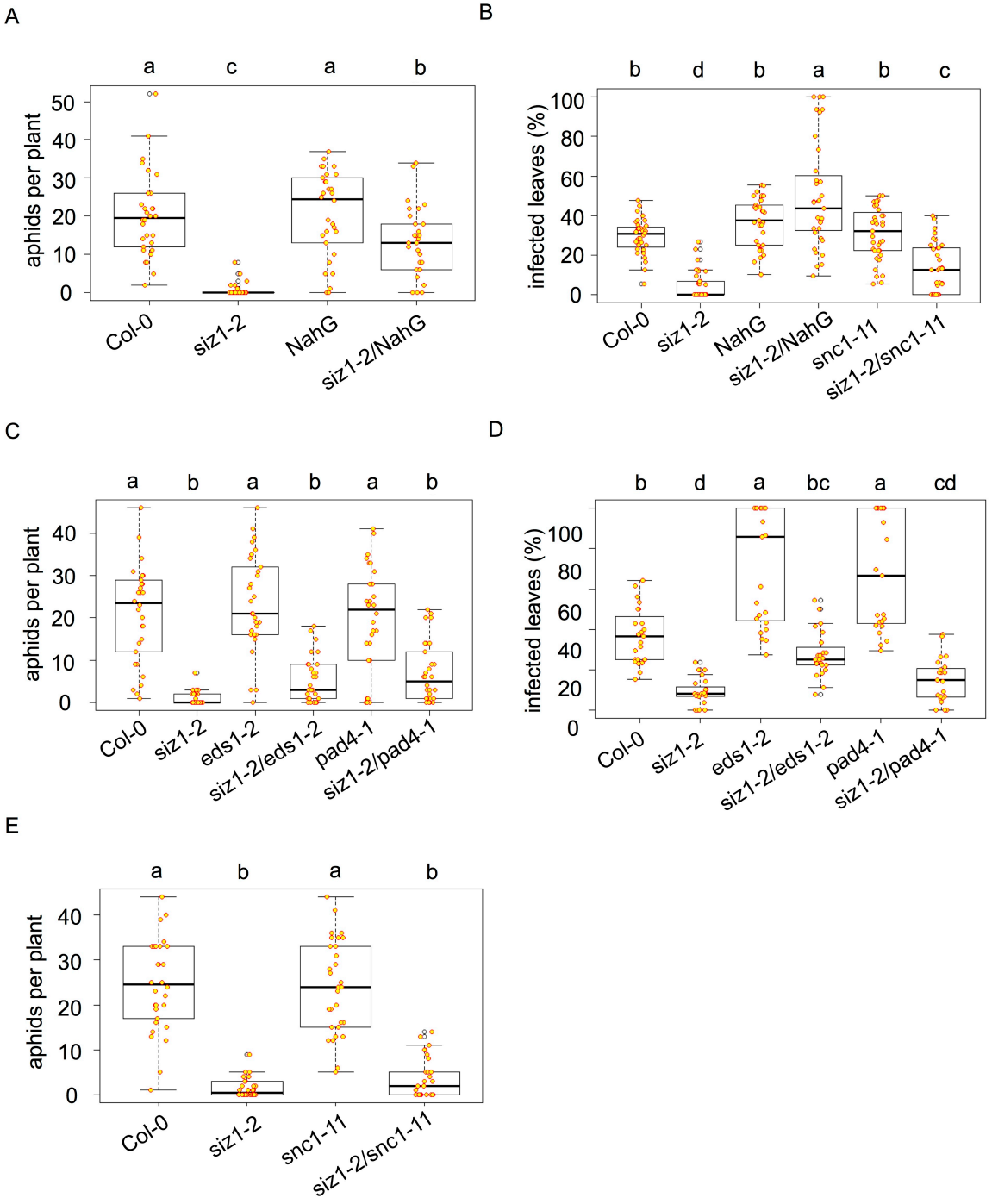

Fig. 6. The Arabidopsis *siz1-2* mutant shows reduced susceptibility to *Myzus persicae* and enhanced resistance to *Phytophthora capsici*.

For aphid infestation assays (A, C, E) plants were infested with two 2-day old nymphs and the aphid populations were counted 10 days later. For *P. capsici* infection assays (B, D) plants were spray-inoculated with a zoospore suspension of 100,000 spores/ml and the percentage of symptomatic leaves was recorded 8 days later. A linear mixed effects model with experimental block and biological replicate as random factors was fitted in dataset from aphid fecundity assays. A linear mixed model with biological replicate as random effect was used in dataset of *P. capsici* infection assays. ANOVA was used to analyse the final models and a post-hoc test was performed by calculating the Least Squares Means by using an emmeans package in R. Different letters denote significant differences within a set of different plant genotypes.

(A) Arabidopsis mutant *siz1-2* is less susceptible to *M. persicae* (aphids) than the Col-0 control with significantly less aphids recorded on the mutant versus control plants ($p<0.0001$), including in the *NahG* background ($p<0.01$).

(B) Arabidopsis mutant *siz1-2* shows enhanced resistance to *P. capsici* compared with the Col-0 control, with significantly less infected leaves on the mutant versus control plants ($p<0.0001$). In the *NahG* background, *siz1-2* is associated with increased infection compared to the *NahG* control ($p<0.01$). The *siz1-2/snc1-11* mutant shows enhanced resistance to *P. capsici* compared with the *snc1-11* mutant, with significantly less leaves infected on the double mutant ($p<0.0001$).

(C) Arabidopsis mutants *siz1-2/esd1-2* and *siz1-2/pad4-1* are less susceptible to *M. persicae* (aphids) than the *eds1-2* and *pad4-1* mutants, respectively, with significantly less aphids recorded on the double compared with the single knock-out mutants ($p<0.0001$).

(D) Arabidopsis mutants *siz1-2/eds1-2* and *siz1-2/pad4-1* are more resistant to *P. capsici* than the *eds1-2* and *pad4-1* mutants, respectively, with significantly less leaves infected on the double compared with the single knock-out mutants ($p<0.0001$).

(E) Arabidopsis mutant *siz1-2/snc1-11* is less susceptible to *M. persicae* (aphids) than the compared *snc1-11* mutant, with significantly less aphids recorded on the double mutant ($p<0.0001$).

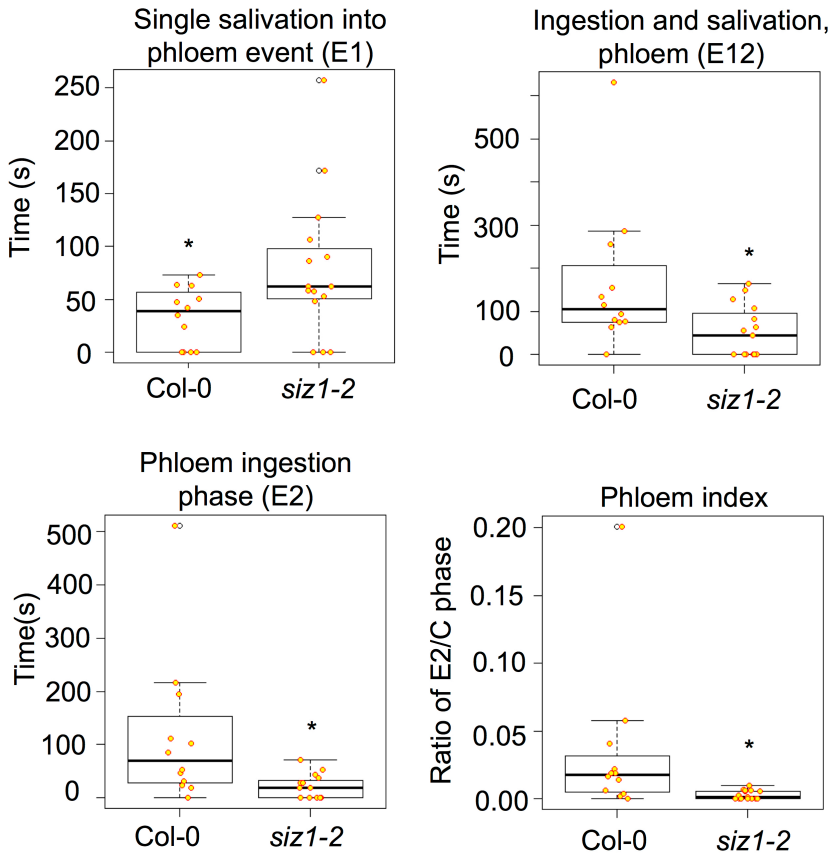

Fig. 7. Aphids show reduced phloem ingestion on the Arabidopsis *siz1-2* mutant. Boxplots show significant EPG parameters indicative of reduced phloem interaction on Arabidopsis *siz1-2* compared with Col-0 plants. E1 phase indicates the phase where aphids secrete saliva into the phloem, E2 phase indicates the phase where aphids ingest phloem sap, E12 phase indicates the phase where aphids either secrete into/ingest phloem, and E2/C ratio indicates the ratio of the time aphids spend on ingesting phloem sap relative to time spend on stylet pathway activities (intercellular). Data was analysed in R studio Version 1.2.5001 running R-3.6.1. Asterisks denote significant difference between the *siz1-2* mutant and Col-0 control (Mann-Whitney U test, $p<0.05$)

Table 1. Overview of significant EPG parameters based on Mann-Whitney U test ($p<0.05$). E1, salivation into phloem; E2, phloem ingestion; E12, fractions of E1 within periods of E1 and E2 waveforms; C, stylet pathway phase, mainly intercellular.

EPG parameter	Hypothesised location of resistance factor	Number of individuals which produced waveform		P value (Mann–Whitney U test)
		Col-0	siz1-2	
All parameters (Global analysis)	All tissue	-	-	0.054
Average duration single E1 period (s)	Phloem	8/12	12/15	0.046
Maximum duration of single E1 period (s)	Phloem	8/12	12/15	0.036
Number of E1 fraction periods	Phloem	11/12	8/15	0.016
Number of E12 periods	Phloem	11/12	8/15	0.017
Average duration of E12 (s)	Phloem	11/12	8/15	0.018
Median duration of E12 (s)	Phloem	11/12	8/15	0.034
Total duration of E12 (s)	Phloem	11/12	8/15	0.006
Maximum duration of E12 (s)	Phloem	11/12	8/15	0.012
Number of E2 periods	Phloem	11/12	8/15	0.017
Average duration of E2 phase (s)	Phloem	11/12	8/15	0.005
Median duration of E2 phase (s)	Phloem	11/12	8/15	0.008
Total duration of E2 phase (s)	Phloem	11/12	8/15	0.003
Maximum duration of E2 phase (s)	Phloem	11/12	8/15	0.005
Time from first E1 phase until first E2 phase (s)	Phloem	12/12	15/15	0.037
Ratio of E2 phase to C phase (%)	Phloem	11/12	8/15	0.002
Ratio of number of E1 fractions to number of E12 (%)	Phloem	11/12	8/15	0.016
Ratio of E2 to total duration after 1st E2 start (%)	Phloem	11/12	8/15	0.006

Supplementary data

Table S1. Candidate interactors of Mp64 and CRN83_152 identified in yeast-two-hybrid screens against a *Nicotiana benthamiana* prey library.

Fig. S1. Amino acid alignment of different versions of SIZ1 and fragments recovered from yeast-two-hybrid screens. Three different prey sequences were recovered for yeast clones from the CRN83_152 screen (11, 18 and 28) and two identical prey sequences were recovered from yeast clones for the Mp64 screen. The CRN83_152 prey clones were only sequenced at the 5'-end. NbSIZ1-cloned corresponds to the NbSIZ1 sequence cloned and used in this study. AtSIZ1 corresponds to AT5G60410.1, NbSIZ1-1 corresponds to Niben101Scf15836g01010.1, NbSIZ1-2 corresponds to Niben101Scf04549g09015.1, Ntom_SIZ1-1 corresponds to XP_018631065.1, Ntom_SIZ1-2 corresponds to XP_018631066.1, NaSIZ1-1 corresponds to XP_019237907.1, NaSIZ1-2 corresponds to XP_019237903.1. Dark blue colour indicates high similarity, light blue colour low similarity.

Fig. S2. Confirmation of interactions between aphid effector Mp64 and AtSIZ1 (Arabidopsis thaliana) or NbSIZ1 (*Nicotiana benthamiana*) in yeast through activation of various reporter genes. Yeast co-transformants were selected on –LT media lacking leucine and tryptophan. -LTH represents selective medium lacking leucine, tryptophan and histidine (-LTH) and -LTHA represents selective medium lacking leucine, tryptophan, histidine and adenine. X-gal assays confirmed activation of the *lacZ* reporter gene. +C and -C indicate the positive and negative controls respectively for reporter activation, and EV indicates bait or prey vector with no insert.

Fig. S3. Mp64 stabilizes SIZ1 *in planta*.

(A) SDS-PAGE gels stained with Coomassie brilliant blue to show equal loading of protein samples for SIZ1 stability assays shown in (B) for 3 biological replicates.

(B Western blot analyses of protein extracts from agroinfiltrated leaves expressing combinations of GFP-GUS, GFP-Mp64 and GFP-CRN83_152_6D10 with AtSIZ1-myc or NbSIZ1-myc. Protein size markers are indicated in kD, and equal protein amounts upon transfer is shown upon ponceau staining (PS) of membranes.

Fig. S4. CRN83-152_6D10 enhances AtSIZ1 triggered cell death in *Nicotiana benthamiana*.

Bar graph showing the proportions of infiltration sites with different levels of cell death upon expression of SIZ1 (with C-terminal RFP tag) either alone or in combination with aphid effector Mp64 or Phytophthora capsica effector CRN83_152_6D10 (both effectors with GFP tag), or a GFP control. Data was collected 4 days after infiltration. Graph represent data from a combination of 2 biological replicates of 11-12 infiltration sites per experiment (n=23). Note that the third biological replicate, not included here, did not yet show cell death symptoms at 4pdi.

Fig. S5. Expression of full length SIZ1-RFP fusion proteins *in planta*.

Western blots showing SIZ1-RFP proteins are expressed as full-length fusion proteins. Leaf samples from infiltration sites in N. benthamiana were collected 3 days after infiltration. Leaf samples were ground in sample buffer and equal amounts were loaded on an SDS-PAGE gel for

western blotting with an RFP-antibody. Marker indicated molecular weight in kD. Ponceau staining shows equal loading and transfer.

Fig. S6. Amino acid alignment of Mp64 and predicted orthologs in aphid species. Mp64-cloned indicates the cloned effector sequence used in this study. Mp64 indicated the *Myzus persicae* database sequences XP_022180025.1. Ap64 indicates the *Acyrthosiphon pisum* sequence XP_008179242.1. Rm64 indicates the *Rhopalosiphum maidis* sequence XP_026817768.1, and Ag64 indicates the *Aphis glycines* sequence KAE9543816.1. Dark blue colour indicates high similarity, light blue colour low similarity. Signal peptide sequence of Mp64 is indicated by a black line. Red boxes indicate predicted SUMOylation sites based on GPS-SUMO 2.0 predictions with medium threshold setting.

Fig. S7. Reverse transcriptase-Polymerase Chain Reaction (RT-PCR) confirms expression of aphid effector Mp64 in transgenic Arabidopsis lines and plant phenotypes.

(A) cDNA from four independent *Arabidopsis thaliana* overexpressing Mp64 lines (20.9, 25.6, 28.11, and 29.5) was used as a template for PCR with primers specific to Mp64 alongside with cDNA from Col-0, plasmid DNA with an Mp64 insert (positive control) and DNAse/RNAse treated water (negative control). The samples were analysed on a 1% agarose gel. The products from the cDNA template and plasmid were detected at the correct size of 274 bp.

(B) Representative images showing the phenotype of two selected Arabidopsis Mp64 transgenic lines (line 25.6 and line 29.5).

Fig. S8. Expression of CRN83_152 but not Mp64 in *Nicotiana benthamiana* enhances host susceptibility to *Phytophthora capsici*. Leaves expressing CRN83_152, Mp64 and vector controls upon agroinfiltration were challenged with 5µl *P. capsici* zoospore suspension (50,000 spores/mL) and the lesion diameter was measured two days post inoculation. A total of 30 infiltration sites per treatment were analyzed (n=30). Asterisks denote significant difference of lesion diameter between the CRN83_152 overexpressing leaves and vector control (Mann-Whitney U test, $p<0.05$).

Fig. S9. Effectors Mp64 and CRN83_152 co-localize with AtSIZ1 in the host nucleus.

Leaves transiently expressing GFP-Mp64, GFP-CRN83_152 or GFP-CRN83_152_6D10 in combination with RFP or AtSIZ1 –RFP were used for confocal imaging 2 days after agroinfiltration. Images show single optical sections through nuclei co-expressing the GFP-effector with AtSIZ1-RFP or RFP control. Scale bars represent 5 µm.

Fig. S10. Virus-induced gene silencing of *NbSIZ1* is effective and reduces host susceptibility to *Phytophthora capsici*.

(A) Representative images showing the phenotype of plants expressing TRV-NbSIZ1 and TRV-GFP-frag. *NbSIZ1*-silenced plants (TRV-NbSIZ1) shows a slightly reduced growth and increased cell death associated virus infection compared to the control (TRV-GFPfrag). TRV-PDS was infiltrated alongside as a positive control.

(B), Lesion diameter was significantly reduced in plants expressing TRV-NbSIZ1 compared to TRV-GFPfrag control. Two biological replicates (n=12 per replicate) were combined in the dataset. *N. benthamiana* leaves were inoculated with 10µl of a *P. capsici* zoospores suspension (100,000

spores/ml). The lesion diameter was recorded four days post inoculation. Asterisks denote significant difference between TRV-NbSIZ1 and TRV-GFPfrag (Mann-Whitney U test, $p<0.001$).

(C) Boxplot showing that the relative expression level of *NbSIZ1* is significantly reduced in *NbSIZ*-silenced plants (TRV-NbSIZ1) compared to control plants (TRV-GFPfrag). RT-qPCR was conducted with three biological replicates. Expression level of NbSIZ1 was normalized against the expression of reference genes *NbPP2A* and *NbEF1α* using $\Delta\Delta$Ct analysis. Asterisks denote significant difference between treatments and control (Mann-Whitney U test, $p<0.0001$)

Fig. S11. Representative images of Arabidopsis mutant lines infected with *Phytophthora capsici*. The plants were spray-inoculated with zoospore suspension of 100,000 spores/ml and the images were taken 8 days post infection.

References

Alvarez AE, Tjallingii WF, Garzo E, Vleeshouwers V, Dicke M, Vosman B (2006) Location of resistance factors in the leaves of potato and wild tuber-bearing Solanum species to the aphid Myzus persicae. Entomologia Experimentalis Et Applicata **121:** 145-157

Amaro TMMM, Thilliez GJA, Mcleod RA, Huitema E (2018) Random mutagenesis screen shows that Phytophthora capsici CRN83_152-mediated cell death is not required for its virulence function(s). Mol Plant Pathol **19:** 1114-1126

Bos JI, Prince D, Pitino M, Maffei ME, Win J, Hogenhout SA (2010) A functional genomics approach identifies candidate effectors from the aphid species Myzus persicae (green peach aphid). PLoS Genet **6:** e1001216

Bos JIB, Armstrong MR, Gilroy EM, Boevink PC, Hein I, Taylor RM, Tian ZD, Engelhardt S, Vetukuri RR, Harrower B, Dixelius C, Bryan G, Sadanandom A, Whisson SC, Kamoun S, Birch PRJ (2010) Phytophthora infestans effector AVR3a is essential for virulence and manipulates plant immunity by stabilizing host E3 ligase CMPG1. Proceedings of the National Academy of Sciences of the United States of America **107:** 9909-9914

Boulain H, Legeai F, Guy E, Morlière S, Douglas NE, Oh J, Murugan M, Smith M, Jaquiéry J, Peccoud J, White FF, Carolan JC, Simon JC, Sugio A (2018) Fast Evolution and Lineage-Specific Gene Family Expansions of Aphid Salivary Effectors Driven by Interactions with Host-Plants. Genome Biology and Evolution **10:** 1554-1572

Bustin SA, Benes V, Garson JA, Hellemans J, Huggett J, Kubista M, Mueller R, Nolan T, Pfaffl MW, Shipley GL, Vandesompele J, Wittwer CT (2009) The MIQE guidelines: minimum information for publication of quantitative real-time PCR experiments. Clin Chem **55:** 611-622

Carolan JC, Caragea D, Reardon KT, Mutti NS, Dittmer N, Pappan K, Cui F, Castaneto M, Poulain J, Dossat C, Tagu D, Reese JC, Reeck GR, Wilkinson TL, Edwards OR (2011) Predicted effector molecules in the salivary secretome of the pea aphid (Acyrthosiphon pisum): a dual transcriptomic/proteomic approach. J Proteome Res **10:** 1505-1518

Carolan JC, Fitzroy CI, Ashton PD, Douglas AE, Wilkinson TL (2009) The secreted salivary proteome of the pea aphid Acyrthosiphon pisum characterised by mass spectrometry. Proteomics **9:** 2457-2467

Castro PH, Verde N, Lourenço T, Magalhães AP, Tavares RM, Bejarano ER, Azevedo H (2015) SIZ1-Dependent Post-Translational Modification by SUMO Modulates Sugar Signaling and Metabolism in Arabidopsis thaliana. Plant Cell Physiol **56:** 2297-2311

Castro PH, Verde N, Tavares RM, Bejarano ER, Azevedo H (2018) Sugar signaling regulation by arabidopsis SIZ1-driven sumoylation is independent of salicylic acid. Plant Signal Behav **13:** e1179417

Catala R, Ouyang J, Abreu IA, Hu Y, Seo H, Zhang X, Chua NH (2007) The Arabidopsis E3 SUMO ligase SIZ1 regulates plant growth and drought responses. Plant Cell **19:** 2952-2966

Chaudhary R, Peng HC, He J, MacWilliams J, Teixeira M, Tsuchiya T, Chesnais Q, Mudgett MB, Kaloshian I (2019) Aphid effector Me10 interacts with tomato TFT7, a 14-3-3 isoform involved in aphid resistance. New Phytologist **221:** 1518-1528

Cheong MS, Park HC, Hong MJ, Lee J, Choi W, Jin JB, Bohnert HJ, Lee SY, Bressan RA, Yun DJ (2009) Specific domain structures control abscisic acid-, salicylic acid-, and stress-mediated SIZ1 phenotypes. Plant Physiol **151:** 1930-1942

Diaz-Granados A, Sterken MG, Persoon J, Overmars H, Pokhare SS, Mazur MJ, Martin-Ramirez S, Holterman M, Martin EC, Pomp R, Finkers-Tomczak A, Roosien J, Elashry A, Grundler F, Petrescu AJ, Smant G, Goverse A (2019) SIZ1 is a nuclear target of the nematode effector GpRbp1 from Globodera pallida that acts as a negative regulator of basal plant defense to cyst nematodes. bioRxiv

Goodin MM, Chakrabarty R, Banerjee R, Yelton S, Debolt S (2007) New gateways to discovery. Plant Physiol **145:** 1100-1109

Gou M, Huang Q, Qian W, Zhang Z, Jia Z, Hua J (2017) Sumoylation E3 Ligase SIZ1 Modulates Plant Immunity Partly through the Immune Receptor Gene SNC1 in Arabidopsis. Mol Plant Microbe Interact **30:** 334-342

Hammoudi V, Fokkens L, Beerens B, Vlachakis G, Chatterjee S, Arroyo-Mateos M, Wackers PFK, Jonker MJ, van den Burg HA (2018) The Arabidopsis SUMO E3 ligase SIZ1 mediates the temperature dependent trade-off between plant immunity and growth. PLoS Genet **14:** e1007157

Hotson A, Chosed R, Shu H, Orth K, Mudgett MB (2003) Xanthomonas type III effector XopD targets SUMO-conjugated proteins in planta. Mol Microbiol **50:** 377-389

Howe GA, Jander G (2008) Plant immunity to insect herbivores. Annu Rev Plant Biol **59:** 41-66

Huot B, Yao J, Montgomery BL, He SY (2014) Growth-defense tradeoffs in plants: a balancing act to optimize fitness. Mol Plant **7:** 1267-1287

Ishida T, Yoshimura M, Miura K, Sugimoto K (2012) MMS21/HPY2 and SIZ1, two Arabidopsis SUMO E3 ligases, have distinct functions in development. PLoS One **7:** e46897

Jin JB, Jin YH, Lee J, Miura K, Yoo CY, Kim WY, Van Oosten M, Hyun Y, Somers DE, Lee I, Yun DJ, Bressan RA, Hasegawa PM (2008) The SUMO E3 ligase, AtSIZ1, regulates flowering by controlling a salicylic acid-mediated floral promotion pathway and through affects on FLC chromatin structure. Plant J **53:** 530-540

Jones JD, Dangl JL (2006) The plant immune system. Nature **444:** 323-329

Kaloshian I, Walling LL (2016) Hemipteran and dipteran pests: Effectors and plant host immune regulators. J Integr Plant Biol **58:** 350-361

Karimi M, Inzé D, Depicker A (2002) GATEWAY vectors for Agrobacterium-mediated plant transformation. Trends in Plant Science **7:** 193-195

Kim JG, Taylor KW, Hotson A, Keegan M, Schmelz EA, Mudgett MB (2008) XopD SUMO protease affects host transcription, promotes pathogen growth, and delays symptom development in xanthomonas-infected tomato leaves. Plant Cell **20:** 1915-1929

Lee J, Nam J, Park HC, Na G, Miura K, Jin JB, Yoo CY, Baek D, Kim DH, Jeong JC, Kim D, Lee SY, Salt DE, Mengiste T, Gong Q, Ma S, Bohnert HJ, Kwak SS, Bressan RA, Hasegawa PM, Yun DJ (2007) Salicylic acid-mediated innate immunity in Arabidopsis is regulated by SIZ1 SUMO E3 ligase. Plant J **49:** 79-90

Lei J, A Finlayson S, Salzman RA, Shan L, Zhu-Salzman K (2014) BOTRYTIS-INDUCED KINASE1 Modulates Arabidopsis Resistance to Green Peach Aphids via PHYTOALEXIN DEFICIENT4. Plant Physiol **165:** 1657-1670

Leybourne DJ, Valentine TA, Robertson JA, Pérez-Fernández E, Main AM, Karley AJ, Bos JI (2019) Defence gene expression and phloem quality contribute to mesophyll and phloem resistance to aphids in wild barley. J Exp Bot

Lin XL, Niu D, Hu ZL, Kim DH, Jin YH, Cai B, Liu P, Miura K, Yun DJ, Kim WY, Lin R, Jin JB (2016) An Arabidopsis SUMO E3 Ligase, SIZ1, Negatively Regulates Photomorphogenesis by Promoting COP1 Activity. PLoS Genet **12:** e1006016

Liu C, Yu H, Li L (2019) SUMO modification of LBD30 by SIZ1 regulates secondary cell wall formation in Arabidopsis thaliana. PLoS Genet **15:** e1007928

Liu D, Shi L, Han C, Yu J, Li D, Zhang Y (2012) Validation of reference genes for gene expression studies in virus-infected Nicotiana benthamiana using quantitative real-time PCR. PLoS One **7:** e46451

Livak KJ, Schmittgen TD (2001) Analysis of relative gene expression data using real-time quantitative PCR and the 2(-Delta Delta C(T)) Method. Methods **25:** 402-408

Lozano-Torres JL, Wilbers RH, Gawronski P, Boshoven JC, Finkers-Tomczak A, Cordewener JH, America AH, Overmars HA, Van 't Klooster JW, Baranowski L, Sobczak M, Ilyas M, van der Hoorn RA, Schots A, de Wit PJ, Bakker J, Goverse A, Smant G (2012) Dual disease resistance mediated by the immune receptor Cf-2 in tomato requires a common virulence target of a fungus and a nematode. Proc Natl Acad Sci U S A **109:** 10119-10124

Lu R, Martin-Hernandez AM, Peart JR, Malcuit I, Baulcombe DC (2003) Virus-induced gene silencing in plants. Methods **30:** 296-303

Mafurah JJ, Ma H, Zhang M, Xu J, He F, Ye T, Shen D, Chen Y, Rajput NA, Dou D (2015) A Virulence Essential CRN Effector of Phytophthora capsici Suppresses Host Defense and Induces Cell Death in Plant Nucleus. PLoS One **10:** e0127965

Mayoral AM, Tjallingii WF, Castanera P (1996) Probing behaviour of Diuraphis noxia on five cereal species with different hydroxamic acid levels. Entomologia Experimentalis Et Applicata **78:** 341-348

Medina-Ortega KJ, Walker GP (2015) Faba bean forisomes can function in defence against generalist aphids. Plant Cell and Environment **38:** 1167-1177

Miura K, Jin JB, Lee J, Yoo CY, Stirm V, Miura T, Ashworth EN, Bressan RA, Yun DJ, Hasegawa PM (2007) SIZ1-mediated sumoylation of ICE1 controls CBF3/DREB1A expression and freezing tolerance in Arabidopsis. Plant Cell **19:** 1403-1414

Miura K, Lee J, Jin JB, Yoo CY, Miura T, Hasegawa PM (2009) Sumoylation of ABI5 by the Arabidopsis SUMO E3 ligase SIZ1 negatively regulates abscisic acid signaling. Proc Natl Acad Sci U S A **106:** 5418-5423

Miura K, Lee J, Miura T, Hasegawa PM (2010) SIZ1 controls cell growth and plant development in Arabidopsis through salicylic acid. Plant Cell Physiol **51:** 103-113

Miura K, Rus A, Sharkhuu A, Yokoi S, Karthikeyan AS, Raghothama KG, Baek D, Koo YD, Jin JB, Bressan RA, Yun DJ, Hasegawa PM (2005) The Arabidopsis SUMO E3 ligase SIZ1 controls phosphate deficiency responses. Proc Natl Acad Sci U S A **102:** 7760-7765

Monaghan J, Zipfel C (2012) Plant pattern recognition receptor complexes at the plasma membrane. Curr Opin Plant Biol **15:** 349-357

Mukhtar MS, Carvunis AR, Dreze M, Epple P, Steinbrenner J, Moore J, Tasan M, Galli M, Hao T, Nishimura MT, Pevzner SJ, Donovan SE, Ghamsari L, Santhanam B, Romero V, Poulin MM, Gebreab F, Gutierrez BJ, Tam S, Monachello D, Boxem M, Harbort CJ, McDonald N, Gai L, Chen H, He Y, Vandenhaute J, Roth FP, Hill DE, Ecker JR, Vidal M, Beynon J, Braun P, Dangl JL, Consortium EUE (2011) Independently evolved virulence effectors converge onto hubs in a plant immune system network. Science **333:** 596-601

Nakagawa T, Suzuki T, Murata S, Nakamura S, Hino T, Maeo K, Tabata R, Kawai T, Tanaka K, Niwa Y, Watanabe Y, Nakamura K, Kimura T, Ishiguro S (2007) Improved Gateway binary vectors: high-performance vectors for creation of fusion constructs in transgenic analysis of plants. Biosci Biotechnol Biochem **71:** 2095-2100

Nguyen Ba AN, Pogoutse A, Provart N, Moses AM (2009) NLStradamus: a simple Hidden Markov Model for nuclear localization signal prediction. BMC Bioinformatics **10:** 202

Pegadaraju V, Louis J, Singh V, Reese JC, Bautor J, Feys BJ, Cook G, Parker JE, Shah J (2007) Phloem-based resistance to green peach aphid is controlled by Arabidopsis PHYTOALEXIN DEFICIENT4 without its signaling partner ENHANCED DISEASE SUSCEPTIBILITY1. Plant Journal **52:** 332-341

Pieterse CM, Van der Does D, Zamioudis C, Leon-Reyes A, Van Wees SC (2012) Hormonal modulation of plant immunity. Annu Rev Cell Dev Biol **28:** 489-521

Rao W, Zheng X, Liu B, Guo Q, Guo J, Wu Y, Shangguan X, Wang H, Wu D, Wang Z, Hu L, Xu C, Jiang W, Huang J, Shi S, He G (2019) Secretome Analysis and In Planta Expression of Salivary Proteins Identify Candidate Effectors from the Brown Planthopper Nilaparvata lugens. Mol Plant Microbe Interact **32:** 227-239

Rasool B, McGowan J, Pastok D, Marcus SE, Morris JA, Verrall SR, Hedley PE, Hancock RD, Foyer CH (2017) Redox Control of Aphid Resistance through Altered Cell Wall Composition and Nutritional Quality. Plant Physiol **175:** 259-271

Ratcliff F, Martin-Hernandez AM, Baulcombe DC (2001) Technical Advance. Tobacco rattle virus as a vector for analysis of gene function by silencing. Plant J **25:** 237-245

Rodriguez PA, Escudero-Martinez C, Bos JI (2017) An Aphid Effector Targets Trafficking Protein VPS52 in a Host-Specific Manner to Promote Virulence. Plant Physiology **173:** 1892-1903

Rytz TC, Miller MJ, McLoughlin F, Augustine RC, Marshall RS, Juan YT, Charng YY, Scalf M, Smith LM, Vierstra RD (2018) SUMOylome Profiling Reveals a Diverse Array of Nuclear Targets Modified by the SUMO Ligase SIZ1 during Heat Stress. Plant Cell **30:** 1077-1099

Singh V, Louis J, Ayre BG, Reese JC, Pegadaraju V, Shah J (2011) TREHALOSE PHOSPHATE SYNTHASE11-dependent trehalose metabolism promotes Arabidopsis thaliana defense against the phloem-feeding insect Myzus persicae. Plant J **67:** 94-104

Song J, Win J, Tian M, Schornack S, Kaschani F, Ilyas M, van der Hoorn RA, Kamoun S (2009) Apoplastic effectors secreted by two unrelated eukaryotic plant pathogens target the tomato defense protease Rcr3. Proc Natl Acad Sci U S A **106:** 1654-1659

Stam R, Howden AJ, Delgado-Cerezo M, M M Amaro TM, Motion GB, Pham J, Huitema E (2013) Characterization of cell death inducing Phytophthora capsici CRN effectors suggests diverse activities in the host nucleus. Front Plant Sci **4:** 387

Stam R, Motion GB, Boevink P, Huitema E (2013) A conserved oomycete CRN effector targets and modulates tomato TCP14-2 to enhance virulence. bioRxiv

Thorpe P, Cock PJA, Bos J (2016) Comparative transcriptomics and proteomics of three different aphid species identifies core and diverse effector sets. Bmc Genomics **17**

Thorpe P, Escudero-Martinez CM, Cock PJA, Eves-van den Akker S, Bos JIB (2018) Shared transcriptional control and disparate gain and loss of aphid parasitism genes. Genome Biology and Evolution

Tjallingii WF (1978) ELECTRONIC RECORDING OF PENETRATION BEHAVIOR BY APHIDS. Entomologia Experimentalis Et Applicata **24:** 721-730

Tjallingii WF (1988) Electrical Recording of Stylet Penetration Activities. *In* AK Minks, P Harrewijn, eds, Aphids Their Biology, Natural Enemies and Control. Elsevier, Amsterdam, Netherlands, pp 95-108

Verma V, Croley F, Sadanandom A (2018) Fifty shades of SUMO: its role in immunity and at the fulcrum of the growth-defence balance. Mol Plant Pathol **19:** 1537-1544

Wang N, Zhao P, Ma Y, Yao X, Sun Y, Huang X, Jin J, Zhang Y, Zhu C, Fang R, Ye J (2019) A whitefly effector Bsp9 targets host immunity regulator WRKY33 to promote performance. Philos Trans R Soc Lond B Biol Sci **374:** 20180313

Wang Y, Bouwmeester K, van de Mortel JE, Shan W, Govers F (2013) A novel Arabidopsis-oomycete pathosystem: differential interactions with Phytophthora capsici reveal a role for camalexin, indole glucosinolates and salicylic acid in defence. Plant Cell Environ **36:** 1192-1203

Weßling R, Epple P, Altmann S, He Y, Yang L, Henz SR, McDonald N, Wiley K, Bader KC, Gläßer C, Mukhtar MS, Haigis S, Ghamsari L, Stephens AE, Ecker JR, Vidal M, Jones JD, Mayer KF, Ver Loren van Themaat E, Weigel D, Schulze-Lefert P, Dangl JL, Panstruga R, Braun P (2014) Convergent targeting of a common host protein-network by pathogen effectors from three kingdoms of life. Cell Host Microbe **16:** 364-375

Will T, van Bel AJE (2006) Physical and chemical interactions between aphids and plants. Journal of Experimental Botany **57:** 729-737

Xu HX, Qian LX, Wang XW, Shao RX, Hong Y, Liu SS (2019) A salivary effector enables whitefly to feed on host plants by eliciting salicylic acid-signaling pathway. Proc Natl Acad Sci U S A **116:** 490-495

Yachdav G, Kloppmann E, Kajan L, Hecht M, Goldberg T, Hamp T, Hönigschmid P, Schafferhans A, Roos M, Bernhofer M, Richter L, Ashkenazy H, Punta M, Schlessinger A, Bromberg Y, Schneider R, Vriend G, Sander C, Ben-Tal N, Rost B (2014) PredictProtein--an open resource for online prediction of protein structural and functional features. Nucleic Acids Res **42:** W337-343

Zhao Q, Xie Y, Zheng Y, Jiang S, Liu W, Mu W, Liu Z, Zhao Y, Xue Y, Ren J (2014) GPS-SUMO: a tool for the prediction of sumoylation sites and SUMO-interaction motifs. Nucleic Acids Res **42:** W325-330